Journal of Proteomics 209 (2019) 103525

Contents lists available at ScienceDirect

Journal of Proteomics

journal homepage: www.elsevier.com/locate/jprot

Proteomic analysis of soluble proteins retrieved from *Duttaphrynus melanostictus* skin secretion by IEx-batch sample preparation

Douglas O.C. Mariano[a], José Pedro Prezotto-Neto[b], Patrick J. Spencer[b], Juliana Mozer Sciani[c], Daniel C. Pimenta[a,*]

[a] Laboratório de Bioquímica e Biofísica, Instituto Butantan, São Paulo, SP 05503-900, Brazil
[b] Centro de Biotecnologia, IPEN, São Paulo, SP 05508-000, Brazil
[c] Laboratório Multidisciplinar de Pesquisa, Universidade São Francisco, Bragança Paulista, SP 12916-900, Brazil

ARTICLE INFO

Keywords:
Amphibian skin secretion
Bufonidae
Duttaphrynus melanostictus
Ion-exchange chromatography
Proteomics
Sample processing

ABSTRACT

Amphibians display a toxic secretion that works as chemical defenses against predators and/or microorganisms that is stored in specialized glands located in the tegument. For some animals, such glands have accumulated in specific regions of the body and formed prominent structures known as macroglands. The Bufonidae family displays conspicuous macroglands in a post-orbital position, termed parotoids, which secretions are known to be extremely viscous and rich in alkaloids and steroids. Few proteins have been described in this material, though. Mainly, because of the difficulties to handle such biological matrix. In this context, we have performed a proteomic study on the parotoid macrogland secretion of the Asian bufonid *Duttaphrynus melanostictus*. By employing the Ion-Exchange (IEx)-batch chromatography (anionic, cationic and both) we obtained six fractions - bound and unbound – that were submitted to an in solution-trypsin digestion followed by LC-MS/MS. Proteins related to: antioxidant activity, binding processes (carbohydrate/lipid/protein), energy metabolism, hydrolases, lipid metabolism and membrane traffic were identified. Moreover, IEx was able to preserve the biological activity of the retrieved proteins (peptidasic). The current study increases the knowledge on the proteins present in the bufonids parotoid macrogland secretion, providing a better understanding of the physiological role played by such molecules.

Significance: The current approach allowed a detailed proteomic analysis of the several proteins synthesized in the *D. melanostictus* parotoid macrogland (Bufonidae) that are secreted into the skins, but embedded within a complex viscous biological matrix. Moreover, our results aim to increase the knowledge on the biological role played by such proteins at the skin.

1. Introduction

The Amphibian integument participates in important physiological processes, such as the ionic and osmotic balances, thermoregulation and defense/protection [1–3]. In the skin, there are specialized glands termed granular (or venom) glands that store a high diversity of biomolecules like alkaloids, peptides, proteins and steroids [3–5]. Once released, the gland's secretion acts as a chemical defense against predators or pathogens [5–8].

Bufonids (Anura: Bufonidae) possess conspicuous protuberances in a post-orbital position termed parotoid macroglands [9,10]. This structure is formed by the grouping of several granular glands and stores a huge quantity and diversity of molecules including alkaloids and steroids [10–12], as well as proteins [10,13,14]. Rash et al. [15] showed the presence of peptides in *Rhinella marina* parotoid macrogland secretion; however, in very low abundance. These authors have suggested that these peptides are derived from housekeeping protein cleavages, i.e., cellular *debris*, and are not major biological active peptides.

Once released, the bufonids parotoid macrogland secretion becomes difficult to handle. This matrix is viscous and, partially, water insoluble [13,16,17], characteristics that impairs – in part - its biochemical characterization studies. Sample preparation steps, on the other hand, like centrifugation, filtration, liquid-liquid extraction or solubilization in organic solvents have allowed studying the alkaloids and steroids contents of this material [11,12,18].

Researchers, though, have assessed different methodological approaches to study the proteins in the bufonid parotoid macrogland

* Corresponding author.
E-mail address: dcpimenta@butantan.gov.br (D.C. Pimenta).

https://doi.org/10.1016/j.jprot.2019.103525
Received 4 July 2019; Received in revised form 15 August 2019; Accepted 12 September 2019
Available online 14 September 2019
1874-3919/

secretion. For example, through an 8KDa cut-off filter dialysis of the *R. schneideri* parotoid macrogland secretion, Sousa-Filho et al. [19] obtained 104 proteins by proteomic analysis. Theses authors described several structural proteins; however, this material exhibited no proteolytic activity. In another study, Kowalski et al. [20] identified 13 proteins after obtaining a methanolic extract of *Bufo bufo* parotoid macrogland secretion.

Recently, our group proposed a new methodological approach to study the proteins from the bufonids parotoid macrogland secretion [21]. We successfully retrieved soluble protein fractions from the Asian common toad *Duttaphrynus melanostictus*. These protein fractions were then proteomically characterized, and a total of forty-two proteins could be identified, as well as 153 peptides were de novo sequenced [22].

In this context, we have now performed a thorough proteomic analysis of the *D. melanostictus* parotoid macrogland secretion by expanding the IEx sample preparation steps, aiming to retrieve the largest possible diversity of proteins present in the secretion. Furthermore, by analyzing our results, we could correlate the annotated biological roles of the identified proteins with the anuran chemical defense/physiology context.

2. Material and methods

2.1. Reagents

All employed reagents were purchased from Sigma Co. (St. Louis, MO, USA). QAE-Sephadex A-25 and SP-Sephadex C-25 were from Pharmacia Fine Chemicals AB Uppsala, Sweden. pH test strip (pH-Fix 0–14) was purchased from Macherey-Nagel, Germany.

2.2. Skin secretion collection

D. melanostictus parotoid macrogland secretion was kindly provided by Venom Supplies Pty ltd., Australia. Anurans from Bali, Indonesia, were collected and the secretion was obtained by squeezing *D. melanostictus* parotoid macrogland. All collected secretion was pooled and lyophilized.

2.3. Ion exchange (IEx) batch chromatography

2.3.1. Anionic exchange

Anionic Exchange (AE) sample preparation was conducted according to Mariano et al. [21], employing 102 mg of *D. melanostictus* parotoid macrogland secretion. Briefly, after the sample-resin incubation step, the anionic salt-displaced fraction (A-SDF) and anionic acid-displaced fraction (A-ADF) could be obtained. Then, we lyophilized the anionic unbound fraction (A-UBF) and submitted it to a Cationic Exchange (CE) sample preparation (below).

2.3.2. Cationic exchange

Based on the protocol developed by Mariano et al. [21] for AE, we proposed a new protocol for Cationic Exchange (CE), as follows. For this batch chromatography, two starting materials were employed: the crude *D. melanostictus* parotoid macrogland secretion (101.2 mg) and the A-UBF (obtained according to the procedure described in 2.3.1).

- Step 1 - **Resin preparation:** we resuspended 0.5 g of SP-Sephadex C-25 resin in 12.5 mL of 50 mM acetic acid (pH 4) and kept the tube, on stand at room temperature, for 18 h. The tube was centrifuged - 500 x*g*, for 5 min - and the supernatant was discarded. After that, we added 12.5 mL of 50 mM acetic acid (pH 4), homogenized for 30 min, using a tube homogenizer, at room temperature, centrifuged i (500 x*g*, 5 min) and the supernatant was discarded. We repeated this last step twice.

- Step 2 - **Sample preparation:** We resuspended *D. melanostictus* lyophilized parotoid macrogland secretion in 20 mL of 50 mM acetic acid (pH 4). We kept the material under constant agitation, followed by sonication, until most of the sample was 'soluble'.

- Step 3 - **Unbound Fraction:** We transferred the parotoid macrogland secretion to the tube containing the cationic resin and kept it under constant homogenization for 1 h, at room temperature. After that, the tube was centrifuged (500 x*g*, for 5 min), the supernatant was removed and termed 'cationic unbound fraction' (C-UBF). We repeated this process twice, and all supernatants were polled.

- Step 4 – **Salt fraction:** Following the removal of C-UBF, we added to the tube 50 mM acetic acid, containing 2 M NaCl (pH 4). This step was conducted as described in step 3: homogenization (1 h), centrifugation (500 x*g*, for 5 min) and supernatant collection. Supernatants were pooled and termed 'cationic salt-displaced fraction' (C-SDF).

- Step 5 – **Basic fraction:** Finally, we added ~50 mM ammonium acetate (pH ~ 7.5–8, as estimated by a pH test strip after ammonium bicarbonate addition to the acetic acid solution). The procedure twice: homogenization (1 h), centrifugation (500 × *g*, during 5 min) and supernatant collection. Supernatants were pooled and termed 'cationic basic-displaced fraction' (C-BDF).

The fractions collected after submiting A-UBF to CE were termed: 'anionic-cationic unbound fraction' (AC-UBF), 'anionic-cationic salt-displaced fraction' (AC-SDF) and 'anionic-cationic basic-displaced fraction' (AC-BDF).

In order to remove insoluble particles, all fractions were mechanically filtered (0.22 μm syringe filters) prior to lyophilization.

2.4. Desalting

Both anionic (A-SDF, A-ADF) and cationic (C-SDF, C-BDF, AC-SDF, AC-BDF) fractions were desalted by using a HiPrep 26/10 desalting column (GE Healthcare) coupled to an AKTA avant 25 preparative system (GE Healthcare). We resuspended each fraction in 5 mL, 25 mM Tris (pH 8.5) and loaded them, individually, into the system. The column was eluted with 25 mM Tris buffer (pH 8.5), at a constant flow rate of 10 mL.min^{-1} and monitored by an UV detector (at 220 and 280 nm) and conductivity. The protein peaks for each sample were collected. After that, all samples were lyophilized.

2.5. Proteomic analysis

2.5.1. In solution digestion

A-SDF, A-ADF, C-SDF, C-BDF, AC-SDF and AC-BDF aliquots were dried. After that, we resuspended each sample in 8 M urea (in 100 mM Tris-HCL, pH 8.5) and Tris(2-carboxyethyl)phosphine hydrochloride (TCEP) (dissolved in water) (20 mM final concentration). The mixtures were kept for 1 h at room temperature. Next, we added iodoacetamide (IAA) (dissolved in water) (10 mM final concentration) and reacted for 1 h, at room temperature, protected from light. Next, we added 100 mM Tris-HCl (pH 8.5), to dilute urea to ≤ 2 M, and 10 μL trypsin (10 ng.μL^{-1} in 100 mM Tris-HCl, pH 8.5). Digestion was carried out for 18 h, at 30 °C. Finally, we stopped the enzymatic reaction by adding 50% ACN / 5% TFA. All samples were dried. Prior to mass spectrometer analyzes, each sample was desalted and the peptides were concentrated by ZipTip® C-18 pipette tips (Millipore). We repeated the ZipTip® C-18 step twice for each sample and pooled them. Samples were dried.

2.5.2. Mass spectrometry (MS) analysis

We resuspended each sample in 5 μL 0.1% formic acid. One μL was automatically injected in a 15 cm × 50 μm Acclaim PepMap™ C-18 column (Thermo Scientific) by a nano chromatography EASY-nLC 1200 system (Thermo Scientific) coupled to an Q Exactive Plus mass spectrometer (Thermo Scientific).

Peptides were eluted at 300 nL.min^{-1}, during 100 min and using a linear gradient of 4–40% B (mobile phase A: 0.1% formic acid (FA) (1:999, *v*/v); mobile phase B: 0.1% FA in 80% acetonitrile (1800:19, v/v/v)). Spray voltage was set at 2.5 kV. The mass spectrometer was operated in data dependent mode, in which one full MS scan was

Table 1
Summary of the experimental approaches, results and tables obtained after IEx-batch sample processing of D. melanostictus parotoid macrogland secretion.

Batch chromatography fraction	Sample code	Related table	Number of identified proteins[a]	Related graphical analysis	Related supplemental material	Number of identified proteins[b]
Salt displaced anion exchange	A - SDF	2	55	Fig. 1 A, B	1	129
Acid displaced anion exchange	A - ADF	3	90[c]	Fig. 1C, D	–	–
Salt displaced cation exchange	C– SDF	4	43	Fig. 2A, B	2	139
Basic displaced cation exchange	C – BDF	5	50	Fig. 2C, D	3	109
Salt displaced anion - cation exchange	AC- SDF	6	23	Fig. 3A, B	4	58
Basic displaced anion - cation exchange	AC – BDF	7	11	Fig. 3C, D	5	30

[a] Proteins identified in two independent experiments.
[b] Proteins identified only in one of the independent experiment (mental material).
[c] Data obtained from a single experiment.

acquired in the *m/z* range of 300–1500 followed by MS/MS acquisition using high energy collision dissociation (HCD) of the ten most intense ions from the MS scan. MS and MS/MS spectra were acquired in the Orbitrap analyzer at 70,000 and 17,500 resolution (at 200 *m/z*), respectively. The maximum injection time and AGC target were set to 25 ms and 3×10^6 for full MS, and 40 ms and 10^5 for MS/MS. The minimum signal threshold to trigger fragmentation event, isolation window and normalized collision energy (NCE) were set to, respectively, 2.5×10^4 cps, 1.4 *m/z* and 28. We applied a dynamic peak exclusion to avoid selecting the same m/z for the next 30 s.

2.5.3. Data processing

RAW files were directly loaded in the software Peaks Studio V7.0 (BSI, Canada). We processed the data for proteomic identification according to the following parameters: MS and MS/MS error mass were 10 ppm and 0.01 Da, respectively; methionine oxidation and carbamidomethylation as variable and fixed modification, respectively; trypsin as cleavage enzyme; maximum missed cleavages (3), maximum variable PTMs per peptide (3) and non-specific cleavage (both); the false discovery rate was adjusted to $\leq 0.5\%$; only proteins with score ≥ 30 and containing at least 1 unique peptide were considered in this study. We analyzed all data against an Amphibia protein database (167,530 entries) compiled on Sep/17 and built by retrieving all UniProt entries associated with this taxon.

2.5.4. Data analysis

We performed two independent experiments for each fraction: A-SDF, C-SDF, C-BDF, AC-SDF and AC-BDF. However, for A-ADF, due to unknown methodological issues, the duplicate is missing.

Proteomic data were analyzed according to the following rationale: I) proteins identified in both experiments; II) proteins identified only in one experiment displaying, however, unequivocal identification and/or relevant biological role. These criteria were based on the absence or presence of the same "UniProtKB accession number" and "UniProtKB entry name" for each protein in both experiments. We only kept in the study proteins containing at least one unique peptide in common in spite similar "UniProtKB entry name" or different "UniProtKB entry name" for it may suggest the presence of isoforms.

Moreover, we only listed one protein for each "protein group" (proteins identified by a common set of peptides - Peaks software classification). The others protein present in the group were considered redundant and removed from the study.

For the 'uncharacterized protein' annotations, a basic local alignment search tool (BLAST) was performed, limiting the search to Amphibia class (taxid: 8292). The highest score alignment for each protein was chosen as the probable correct annotation.

2.6. Hydrolase activity

We performed a zymography adapted from Heussen and Dowdle (1980) [23], using casein (2 mg.mL^{-1}) as substrate. Casein were incorporated in a 12% resolving gel with a 4% stacking gel without the substrate. An aliquot of each sample was lyophilized and resuspended in non-reducing sample buffer (0.0625 M Tris (pH 6.8), 10% glycerol, 2% SDS and 0.02% bromophenol blue) and loaded in the gel. After electrophoresis, the SDS was removed by washing the gel twice, for 20 min, in 2.5% Triton X-100. Subsequently, the gel was incubated in 20 mM Tris, 0.5 mM calcium chloride (pH 7.4), at 37C, during 16 h. Besides that, the gel was stained in a solution of acetic acid/methanol/water (10/45/45, *v*/v/v) containing 0.125% Coomassie Brilliant Blue R-250. The gel was destained in a solution of acetic acid/ethanol/water (10/43.5/46.5, v/v/v). *Crotalus viridis viridis* (10 ng) venom was used as positive control.

3. Results and discussion

3.1. D. melanostictus IEx-batch chromatography

Since our aim was to perform a broad proteomic analysis of the macrogland protein content, and not to separate/purify proteins from *D. melanostictus* parotoid macrogland secretion, our previously described methodology [21] was employed, with variations, namely: we adapted the methodology to use a cationic resin in the batch sample preparation.

According to our sample processing approach, we generated the following fractions (Table 1).

After proper batch sample preparation via IEx, we identified several proteins:

3.1.1. Anionic batch exchange

55 proteins were identified in A-SDF (Table 2). Other 129 proteins were identified only in one of the duplicates (Supplemental material 1). Regarding the A-ADF sample, 90 proteins were identified (Table 3); however, this sample lacks its duplicate.

3.1.2. Cationic batch exchange

For C-SDF and C-BDF samples, a total of 44 and 50 proteins were identified, respectively (Tables 4–5). Another 139 (C-SDF) and 109 (C-BDF) proteins were only identified in one of the experiments (Supplemental material 2–3).

3.1.3. Anionic-Cationic batch exchange

AC-SDF and AC-BDF fractions showed the lowest protein identification: 23 and 11 proteins, respectively (Tables 6–7); these numbers increase if we look at proteins identified in only one experiment: 58 and 30 proteins in AC-SDF and AC-BDF, respectively (Supplemental material 4–5).

These results reveal that some proteins do elute in A-UBF. Eighteen proteins present in AC-SDF and AC-BDF could not be identified in A-SDF sample processing approach (Table 2 vs Tables 6–7) (since A-ADF

Table 2
Proteins identified in A-SDF fraction.

Accession	Analysis 1			Analysis 2			Average mass (Da)	Description	Organism	Blast alignment		
	-10lgP	Coverage (%)	Identified peptides	-10lgP	Coverage (%)	Identified peptides				Protein	*E*-value	Acession
A4K520	387.14	82	46	218.72	69	17	9905	Diazepam binding inhibitor	*Bufo gargarizans*			
P45883	303.2	58	27	170.58	48	11	9808	Acyl-CoA-binding protein homolog	*Pelophylax ridibundus*			
P56217	271.07	46	24	152.43	33	11	14,711	Galectin-1	*Rhinella arenarum*			
Q7SY90	270.43	15	13	106.07	12	5	60,259	Catalase	*Xenopus laevis*			
Q9PWF7	265.84	17	10	100.24	12	5	60,251	Catalase	*Rugosa rugosa*			
Q4KLC5	250.93	88	22	124.34	26	6	8374	MGC116485 protein	*Xenopus laevis*	Acyl-CoA-binding protein homolog [*Xenopus laevis*]	2.00E-43	XP_018124633.1
Q642N4	247.83	16	8	90.83	7	3	35,907	Ltb4dh protein	*Xenopus tropicalis*			
A0A0U3A3X0	221.43	29	14	113.65	15	5	41,882	Gamma actin	*Bufo gargarizans*			
A0A1L8G6S1	220.74	26	12	110.68	15	3	26,318	Histone H4	*Xenopus laevis*			
Q3KPN6	218.42	39	10	71.13	7	2	29,455	Proteasome subunit alpha type	*Xenopus laevis*			
A4K522	213.48	35	6	91.8	14	2	15,576	Superoxide dismutase [Cu−Zn]	*Bufo gargarizans*			
C1C4P2	212.52	44	7	74.32	21	3	16,838	Calmodulin	*Lithobates catesbeiana*			
Q9PVQ1	209.12	44	10	94.95	13	3	27,935	Proteasome subunit alpha type-7-B	*Xenopus laevis*			
Q6GND4	208.79	19	8	114.79	24	2	9653	Dbib protein	*Xenopus laevis*			
Q28IY4	206.57	22	10	101.63	9	3	40,360	Adenosine kinase	*Xenopus tropicalis*			
C1C413	205.3	68	9	74.05	13	1	11,971	Pterin-4-alpha-carbinolamine dehydratase	*Lithobates catesbeiana*			
Q5XGB0	195.51	13	9	80.86	10	3	35,938	Aldo-keto reductase family 1 member B7	*Xenopus tropicalis*			
Q28EA4	181.76	39	7	53.93	10	1	15,288	Cytochrome b-5	*Xenopus tropicalis*			
A9UMJ8	179.85	5	5	50.2	1	1	117,501	AP2-associated kinase 1	*Xenopus tropicalis*			
A0A1L8GFL4	178.3	11	7	94.63	6	3	37,238	Uncharacterized protein	*Xenopus laevis*	Alcohol dehydrogenase [NADP(+)]-like [*Xenopus laevis*]	0	XP_018116320.1
A0A1L8EZQ1	177.24	32	7	40.1	4	1	26,511	Proteasome subunit alpha type	*Xenopus laevis*			
A4IHI3	172.55	25	4	86.28	12	2	26,418	Proteasome subunit alpha type	*Xenopus tropicalis*			
Q642N1	172.22	23	7	98.57	9	2	29,363	Proteasome subunit alpha type	*Xenopus tropicalis*			
Q28EJ3	166.76	26	7	58.99	6	1	29,056	Tropomyosin 3	*Xenopus tropicalis*			
A4K523	161.34	27	5	93.33	14	3	22,339	Biliverdin reductase B	*Bufo gargarizans*			
A0A1L8GCS1	158.88	12	5	55.59	2	1	62,494	Uncharacterized protein	*Xenopus laevis*	Stress-induced phosphoprotein STI1 [*Xenopus laevis*]	0	AAM77586.1
A4K534	157.78	4	4	57.2	1	1	99,046	Uncharacterized protein	*Bufo gargarizans*	TRPM8 channel-associated factor homolog [*Nanorana parkeri*]	0	XP_018419924.1
P24495	155.04	28	5	69.81	4	1	25,834	Proteasome subunit alpha type-2	*Xenopus laevis*			
Q90ZD6	147.13	35	6	90.5	23	2	13,816	Histone H2A	*Bufo gargarizans*			
F7C920	141.13	3	4	72.79	3	2	36,271	Uncharacterized protein	*Xenopus tropicalis*	Prostaglandin reductase 1-like [*Xenopus laevis*]	0	XP_018099223.1
A0A1L8G977	129.74	8	4	39.71	2	1	65,674	Malic enzyme	*Xenopus laevis*			
C1C4S1	129.13	5	3	59.14	6	2	37,305	Transaldolase	*Lithobates catesbeiana*			
F7DTU8	121.84	9	3	52.33	4	1	37,346	Uncharacterized protein	*Xenopus tropicalis*	3-oxo-5-beta-steroid 4-dehydrogenase [*Xenopus tropicalis*]	0	NP_001025609.1
F7ELE6	115.51	7	4	63.7	8	3	36,901	Aldo-keto reductase family 1 member C8	*Xenopus tropicalis*			
Q6P7M7	111.94	20	4	71.89	9	2	24,761	Proteasome subunit beta type	*Xenopus tropicalis*			
Q6NVJ0	108.11	6	2	30.6	2	1	61,756	Phosphoglucomutase 1	*Xenopus tropicalis*			

(*continued on next page*)

Table 2 (*continued*)

Accession	Analysis 1			Analysis 2			Average mass (Da)	Description	Organism	Blast alignment		
	-10lgP	Coverage (%)	Identified peptides	-10lgP	Coverage (%)	Identified peptides				Protein	*E*-value	Acession
Q5XGB4	103.99	12	2	54.86	5	1	24,921	Brain abundant membrane attached signal protein 1	*Xenopus tropicalis*			
A0A1W6BSU1	103.67	34	3	31.99	9	1	11,348	Myosin light polypeptide 6 (Fragment)	*Plethodon vehiculum*			
Q6DF14	103.24	9	2	45.6	4	1	31,994	Thioredoxin-like 1	*Xenopus tropicalis*			
A0A1L8GZD2	101.73	6	2	51.37	2	1	38,172	Uncharacterized protein	*Xenopus laevis*	Phytanoyl-CoA dioxygenase, peroxisomal-like [*Xenopus laevis*]	0	XP_018108213.1
C1C4D5	101.24	7	2	49.26	7	1	22,011	Myosin light polypeptide 3	*Lithobates catesbeiana*			
A0A1L8HKY2	98.24	7	2	66.9	12	3	25,313	Uncharacterized protein	*Xenopus laevis*	Quinoid dihydropteridine reductase S homeolog [*Xenopus laevis*]	3.00E-173	NP_001089804.1
P28024	97.49	12	3	58.54	6	1	26,759	Proteasome subunit beta type-4 (Fragment)	*Xenopus laevis*			
Q6GLT8	93.65	5	1	49.15	5	1	35,122	Fumarylacetoacetate hydrolase domain-containing protein 2	*Xenopus laevis*			
Q6P7L5	90.11	6	2	57.18	4	1	36,596	L-lactate dehydrogenase	*Xenopus tropicalis*			
G5E164	84.9	10	1	42.29	10	1	14,214	Putative programmed cell death 5 (Fragment)	*Hymenochirus curtipes*			
Q6P3P0	83.21	7	2	41.04	5	1	26,741	EF-hand domain family member D1	*Xenopus tropicalis*			
Q6DF50	77.28	2	1	52.13	2	1	40,201	Core histone macro-H2A	*Xenopus tropicalis*			
F7ESS5	75.51	11	1	52.83	11	1	14,662	Eukaryotic translation initiation factor 6	*Xenopus tropicalis*			
F6UFZ4	70	11	1	56.54	11	1	13,202	Glutathione peroxidase 3	*Xenopus tropicalis*			
A0A1L8HIK9	69.91	1	1	32.36	2	1	68,627	Uncharacterized protein	*Xenopus laevis*	Eukaryotic translation initiation factor 4B [*Xenopus tropicalis*]	0	NP_001005064.1
Q6DF17	68.78	8	1	56.27	8	1	20,219	Progesterone receptor membrane component 1	*Xenopus tropicalis*			
F6X7G4	55.97	4	1	38.6	4	1	29,342	Cathepsin Z	*Xenopus tropicalis*			
A0A1L8FFP2	44.85	1	1	33.12	1	1	103,803	Uncharacterized protein	*Xenopus laevis*	A disintegrin and metalloproteinase with thrombospondin motifs 15-like [*Xenopus laevis*]	0	XP_018083197.1

Table 3
Proteins identified in A-ADF fraction.

Accession	-10lgP	Coverage (%)	Identified peptides	Average mass (Da)	Description	Organism	Blast alignment		
							Protein	*E*-value	Acession
A4K520	336.3	78	21	9905	Diazepam binding inhibitor	*Bufo gargarizans*			
P45883	299.44	49	18	9808	Acyl-CoA-binding protein homolog	*Pelophylax ridibundus*			
Q7SY90	240.62	13	8	60,259	Catalase	*Xenopus laevis*			
Q0VFH2	235.48	57	9	9993	Acyl-CoA-binding domain-containing 7	*Xenopus tropicalis*			
P56217	233.03	33	13	14,711	Galectin-1	*Rhinella arenarum*			
Q9PWF7	221.49	17	9	60,251	Catalase	*Rugosa rugosa*			
Q4KLC5	198.8	58	12	8374	MGC116485 protein	*Xenopus laevis*	acyl-CoA-binding protein homolog [*Xenopus laevis*]	2.00E-43	XP_018124633.1
Q9I9P5	186.6	10	7	56,619	Inner-ear cytokeratin	*Lithobates catesbeiana*			
P0DP34	185.64	44	5	16,838	Calmodulin-2 A	*Xenopus laevis*			
Q90ZF7	183.71	10	7	56,378	Keratin 8	*Lithobates catesbeiana*			
A4K522	181.19	17	5	15,576	Superoxide dismutase [Cu−Zn]	*Bufo gargarizans PE*			
Q5PPP6	178.98	19	4	28,366	Proteasome subunit alpha type	*Xenopus tropicalis*			
A0A0U3A3X0	178.74	16	7	41,882	Gamma actin	*Bufo gargarizans*			
A0A1L8G6S1	170.96	31	8	26,318	Histone H4	*Xenopus laevis*			
Q0IIY0	170.88	7	6	60,558	Keratin 5 gene 2	*Xenopus tropicalis*			
C1C413	159.32	39	5	11,971	Pterin-4-alpha-carbinolamine dehydratase	*Lithobates catesbeiana*			
Q7ZYL1	152.99	20	3	26,635	Proteasome subunit beta type	*Xenopus laevis*			
A0A0M4N4D0	152.81	14	2	20,719	Ferritin	*Andrias davidianus*			
Q6P8E4	147.19	20	3	26,566	Proteasome subunit beta type	*Xenopus tropicalis*			
H6UFK2	141.69	19	3	17,842	Keratin 5 protein 2 (Fragment)	*Spea multiplicata*			
F7DFH2	140.89	6	3	54,631	Keratin 5 gene 3	*Xenopus tropicalis*			
C1C3N9	140.58	28	4	17,975	Ubiquitin	*Lithobates catesbeiana*			
Q5XGB4	135.86	9	3	24,921	Brain abundant membrane attached signal protein 1	*Xenopus tropicalis*			
A0A1L8GFL4	135.64	8	3	37,238	Uncharacterized protein	*Xenopus laevis*	alcohol dehydrogenase [NADP(+)]-like [*Xenopus laevis*]	0	XP_018116320.1
Q642N4	134.02	8	2	35,907	Ltb4dh protein	*Xenopus tropicalis*			
A0A1L8EZQ1	133.76	12	4	26,511	Proteasome subunit alpha type	*Xenopus laevis*			
A0A1L8HXY0	133.43	6	3	44,969	Uncharacterized protein	*Xenopus laevis*	UV excision repair protein RAD23 homolog B [*Xenopus tropicalis*]	0	NP_001082494.1
Q6GND4	132.16	24	2	9653	Dbia protein	*Xenopus laevis*			
G5DY52	130.47	53	5	10,808	Putative 6-pyruvoyl-tetrahydropterin synthase dimerization cofactor of hepatocyte nuclear factor 1 alpha (Fragment)	*Hymenochirus curtipes*			
G5DYZ1	129.53	13	4	21,609	Putative brain membrane attached signal protein 1 (Fragment)	*Hymenochirus curtipes*			
Q66JK8	127.71	11	3	29,499	Proteasome subunit alpha type	*Xenopus tropicalis*			
A4K530	126.13	19	2	13,524	Protein kinase C inhibitor	*Bufo gargarizans*			
Q28EA4	126.08	35	3	15,288	Cytochrome b-5	*Xenopus tropicalis*			
A4K523	123.37	12	2	22,339	Biliverdin reductase B	*Bufo gargarizans*			
C1C4Z2	119.85	13	2	20,775	Ferritin	*Lithobates catesbeiana*			
A0A1L8GCS1	118.33	6	3	62,494	Uncharacterized protein	*Xenopus laevis*	stress-induced phosphoprotein STI1 [*Xenopus laevis*]	0	AAM77586.1
F7ABC2	115.24	16	3	9645	High mobility group nucleosomal binding domain 2	*Xenopus tropicalis*			
A0A1L8HA73	109.73	2	2	56,899	Uncharacterized protein	*Xenopus laevis*	keratin, type II cytoskeletal cochleal-like [*Xenopus laevis*]	0	XP_018104126.1

(*continued on next page*)

Table 3 (*continued*)

Accession	-10lgP	Coverage (%)	Identified peptides	Average mass (Da)	Description	Organism	Blast alignment		
							Protein	*E*-value	Acession
F7CW40	107.63	4	2	33,253	Uncharacterized protein	*Xenopus tropicalis*	prostaglandin reductase 1-like [*Xenopus laevis*]	0	XP_018099223.1
G5DYL6	106	11	2	26,458	Putative tropomyosin 3 (Fragment)	*Hymenochirus curtipes*			
F6VFT5	104.37	6	1	27,742	Proteasome subunit alpha type	*Xenopus tropicalis*			
Q5M999	100.33	9	2	23,030	Proteasome subunit beta type	*Xenopus laevis*			
F6Y6U8	97.48	1	1	97,711	Uncharacterized protein	*Xenopus tropicalis*	calpastatin isoform X15 [*Xenopus tropicalis*]	0	XP_012811560.1
P24495	96.47	9	1	25,834	Proteasome subunit alpha type-2	*Xenopus laevis*			
Q6P7M7	96.2	13	3	24,761	Proteasome subunit beta type	*Xenopus tropicalis*			
Q28IY4	94.23	3	1	40,360	Adenosine kinase	*Xenopus tropicalis*			
G5DZI4	91.89	6	1	27,399	Putative 14–3-3 protein (Fragment)	*Pipa carvalhoi*			
Q6P382	90.17	9	1	12,361	Eukaryotic translation initiation factor 4E binding protein 2	*Xenopus tropicalis*			
F7C7V3	86.93	6	1	24,596	Charged multivesicular body protein 4b	*Xenopus tropicalis*			
C1C4D5	85.08	7	1	22,011	Myosin light polypeptide 3	*Lithobates catesbeiana*			
B7ZU10	80.94	7	2	35,995	Uncharacterized protein	*Xenopus tropicalis*	prostaglandin reductase 1 [*Xenopus tropicalis*]	0	XP_017953051.1
Q5XGB0	77.07	2	1	35,938	Aldo-keto reductase family 1 member B7	*Xenopus tropicalis*			
F6TJ80	75.99	3	2	70,968	Heat shock protein family A (Hsp70) member 1A	*Xenopus tropicalis*			
F6VLB2	75.99	3	2	70,544	Heat shock protein family A (Hsp70) member 1B	*Xenopus tropicalis*			
A0A1L8GB81	75.25	1	1	140,289	Uncharacterized protein	*Xenopus laevis*	zinc finger and BTB domain-containing protein 38-like [*Xenopus laevis*]	0	XP_018119438.1
Q6P358	73.45	2	1	52,722	CNDP dipeptidase 2 (Metallopeptidase M20 family)	*Xenopus tropicalis*			
F7ELE6	73.25	6	2	36,901	Aldo-keto reductase family 1 member C8 pseudogene	*Xenopus tropicalis*			
F5BBG7	72.97	25	1	7682	Superoxide dismutase A (Fragment)	*Rana luteiventris*			
A0A1L8ENL5	72.37	5	1	29,553	Uncharacterized protein	*Xenopus laevis*	insulin-like growth factor-binding protein 5 [*Xenopus laevis*]	0	XP_018094172.1
Q6GP69	71.92	2	1	40,143	Core histone macro-H2A	*Xenopus laevis*			
A0A1L8I1Z7	71.24	1	1	63,065	Beta-hexosaminidase	*Xenopus laevis*			
Q6P624	71.1	5	1	25,156	Peroxiredoxin 6	*Xenopus tropicalis*			
F7CTI1	70.92	3	1	46,714	Vesicle amine transport 1	*Xenopus tropicalis*			
A0A1L8HLJ7	70.46	2	1	49,713	Uncharacterized protein	*Xenopus laevis*	testican-3-like isoform X1 [*Xenopus laevis*]	0	XP_018098712.1
A0A1S6XZG7	70.2	2	1	50,442	Clusterin	*Bufo gargarizans*			
C1C4V2	69.55	5	1	16,360	Elongation factor 1-beta	*Lithobates catesbeiana*			
Q6DFR0	67.13	5	1	30,069	Toll-interacting protein	*Xenopus tropicalis*			
A0A1L8GI87	66.69	4	1	29,991	L-lactate dehydrogenase	*Xenopus laevis*			
Q0VGV3	65.94	16	1	7838	Ribosomal protein S28 pseudogene 9	*Xenopus tropicalis*			
F6QN60	65.33	5	1	23,517	Proteasome subunit alpha type	*Xenopus tropicalis*			
Q6IP73	64.72	7	1	23,206	Nascent polypeptide-associated complex subunit alpha	*Xenopus laevis*			
A0A1W6BSK9	63.89	10	1	9913	Myosin light polypeptide 6 (Fragment)	*Plethodon dunni*			
A0A1L8EQP5	62.56	4	1	39,478	Fructose-bisphosphate aldolase	*Xenopus laevis*			
P28024	61.46	6	1	26,759	Proteasome subunit beta type-4 (Fragment)	*Xenopus laevis*			
F6TRE5	60.61	3	1	62,732	Neurofilament light polypeptide	*Xenopus tropicalis*			
C1C4C8	58.88	6	1	14,502	Prefoldin subunit 6	*Lithobates catesbeiana*			
A0A0K0LFG4	58.57	1	1	66,491	NADH-ubiquinone oxidoreductase chain 5	*Papurana kreffti*			
Q7ZYT4	56.57	2	1	40,653	Nsfl1c protein	*Xenopus laevis*			
C1C4Z9	54.7	4	1	17,274	Transcription factor BTF3	*Lithobates catesbeiana*			
Q6P8C0	52.78	14	1	11,559	High-mobility group nucleosome binding domain 1	*Xenopus tropicalis*			

(*continued on next page*)

Table 3 (*continued*)

Accession	-10lgP	Coverage (%)	Identified peptides	Average mass (Da)	Description	Organism	Blast alignment		
							Protein	*E*-value	Accession
A0A1L8G7W1	49.82	0	1	241,359	Uncharacterized protein	*Xenopus laevis*	AT-rich interactive domain-containing protein 1B-like [*Xenopus laevis*]	0	XP_018118572.1
F8V2T4	48.56	3	1	38,009	Nuclear migration protein	*Xenopus tropicalis*			
F7CIH4	47.62	3	1	57,548	ATP synthase subunit alpha	*Xenopus tropicalis*			
A0A1L8G0V3	46.72	5	1	17,664	Lactoylglutathione lyase	*Xenopus laevis*			
P27006	44.63	4	1	38,545	Annexin A2-A	*Xenopus laevis*			
P24801	44.63	4	1	38,774	Annexin A2-B	*Xenopus laevis*			
P46472	43.09	3	1	48,664	26S proteasome regulatory subunit 7	*Xenopus laevis*			
Q5M8L9	42.77	3	1	23,444	EF-hand domain family member D2	*Xenopus tropicalis*			
C1C3Q9	41.43	5	1	16,987	Ubiquitin-conjugating enzyme E2 L3	*Lithobates catesbeiana*			
A0A1L8GVT4	39.94	4	1	34,366	Eukaryotic translation initiation factor 3 subunit G	*Xenopus laevis*			

do not present an experimental duplicate, we avoided comparison to AC-BDF). Besides, 17 proteins (11 in AC-SDF and 6 in AC-BDF) were not present in C-SDF (Table 4 vs Table 6) and C-BDF (Table 5 vs Table 7). We identified 13 proteins after subsequent anionic and cationic batch processing (Tables 6–7, identified by an asterisk).

The anionic batch processing successfully retrieves several proteins itself, as expected once the method was mainly developed to remove the positively charged alkaloids from the secretion [21] that impair proper proteomic processing. Nevertheless, performing the cationic batch IEx as well increased the protein identification rate.

3.2. *D. melanostictus* overall proteome distribution

Figs. 1–3 present the molecular function of all identified proteins in A-SDF, A-ADF, C-SDF, C-BDF, AC-SDF and AC-BDF (criterion: group I, according to section 2.5.4) based on the Gene Ontology (GO) Project [24]. Proteins were classified, mostly, in three categories: antioxidant activity (inhibition of reactions through dioxygen (O_2) or peroxides), binding (the selective, non-covalent, often stoichiometric, interaction of a molecule with one or more specific sites on another molecule) and catalytic activity (catalysis of a biochemical reaction at physiological temperatures).

3.3. Proteome analysis

Bufonids present granular glands grouped in the post-orbital region termed parotoid macroglands. This macroglands resembles a honeycomb structure, composed by several alveoli disposed side by side [9,25]. Each alveolus corresponds to one granular gland, which internally contain a syncytial secretory unit devoid of lumen and rich in granules disposed in a central position [9,10,25]. Delfino et al. [26] showed that all granular glands studied had “a single row of nuclei that occupies the most peripheral cytoplasm of the secretory syncytium, encircled by peculiar smooth muscle (myoepithelial) cells. The peripheral cytoplasm contains the biosynthesis machinery: Rough Endoplasmic Reticulum (Rer) and Golgi stacks. This layer of organelles encircles the intracytoplasmic secretory product, which as a rule consists of granules.” Due to the syncytial nature of granular gland, it would be expected the ‘contamination’ of certain housekeeping proteins in the secretion, such as actin, tropomyosin, myosin and cytokeratin, for example.

Regardless of sample processing, at least three protein classes were always present in our analyses: i) Antioxidant activity; ii) Binding and; iii) Catalytic activity.

We discuss below their possible biological roles.

3.3.1. Antioxidant activity

The Anuran skin displays a poorly cornified integument, a feature that allows the involvement of the skin in different physiological process [1,2]. Consequently, this organ is more susceptible to external prooxidant agents [27] that promote the production of free radicals and reactive oxygen species (ROS). The same ROS can be formed intracellularly during physiological processes [27].

ROS are capable to induce DNA damage and oxidize lipids and proteins [27,28]. Schuch et al. [29] observed that UV radiation was genotoxic in *Hypsiboas pulchellus*, inducing malformations and reducing tadpole survival.

Peptides showing antioxidant activity have already been identified in anuran skin secretion [30–32]. Besides, proteins related to the antioxidant system were identified in *R. schneideri* parotoid macrogland secretion [19] and in *Dermatonotus muelleri* skin secretion [33].

Here we identified 5 proteins related to antioxidant system after IEx batch chromatography: catalase, glutathione peroxidase 3, peroxiredoxin 6, superoxide dismutase and thioredoxin like 1. These antioxidant enzymes may protect the animal against ROS damage generated *endo*- and exogenously.

Table 4
Proteins identified in C-SDF fraction.

Accession	Analysis 1			Analysis 2			Average mass (Da)	Description	Organism	Blast alignment		
	-10lgP	Coverage (%)	Identified peptides	-10lgP	Coverage (%)	Identified peptides				Protein	*E*-value	Acession
A4K520	263.51	70	19	337.31	84	74	9905	Diazepam binding inhibitor	*Bufo gargarizans*			
A4K522	164.16	32	6	173.43	59	11	15,576	Superoxide dismutase [Cu−Zn]	*Bufo gargarizans*			
P56217	157.69	26	7	181.07	37	16	14,711	Galectin-1	*Rhinella arenarum*			
G5DYZ1	155.75	14	8	80.26	14	2	21,609	Putative brain membrane attached signal protein 1 (Fragment)	*Hymenochirus curtipes*			
M1R8K5	147.6	35	4	163.12	57	10	14,204	Ubiquitin (Fragment)	*Rana clamitans*			
P22844	142.38	17	4	149.23	26	9	21,062	Histone H1.0-B	*Xenopus laevis*			
Q4KLC5	117.31	34	4	196.71	79	26	8374	MGC116485 protein	*Xenopus laevis*	acyl-CoA-binding protein homolog [*Xenopus laevis*]	2.00E-43	XP_018124633.1
Q5XGB4	110.34	12	4	78.92	5	2	24,921	Brain abundant membrane attached signal protein 1	*Xenopus tropicalis*			
C1C3W4	103.1	20	4	140.39	38	12	9994	Acyl-CoA-binding protein	*Lithobates catesbeiana*			
A0A0U3A3X0	88.55	5	3	113.44	13	6	41,882	Gamma actin	*Bufo gargarizans PE*			
Q7SY90	87.54	2	1	176.61	15	13	60,259	Catalase	*Xenopus laevis*			
F7DS59	87.36	8	2	65.71	8	1	22,002	Cellular repressor of E1A-stimulated	*Xenopus tropicalis*			
A0A1L8HIM2	85.35	2	1	53.18	2	1	57,323	Uncharacterized protein	*Xenopus laevis*	keratin, type II cytoskeletal cochleal-like [*Xenopus laevis*]	0	XP_018101046.1
Q6P624	84.46	10	2	84.78	10	3	25,156	Peroxiredoxin 6	*Xenopus tropicalis*			
Q90ZD6	79.94	21	2	149.31	48	7	13,816	Histone H2A	*Bufo gargarizans*			
F7DTR3	79.63	14	2	81.24	8	2	20,344	Uncharacterized protein	*Xenopus tropicalis*	28 kDa heat- and acid-stable phosphoprotein [*Xenopus tropicalis*]	4.00E-124	NP_001107539.1
Q6P7M0	75.17	6	2	57.72	4	1	38,614	Annexin	*Xenopus tropicalis*			
Q7SZ22	73.83	13	1	96.3	55	3	10,713	Small ubiquitin-related modifier 3	*Xenopus laevis*			
Q6P382	73.47	9	1	91.47	13	3	12,361	Eukaryotic translation initiation factor 4E binding protein 2	*Xenopus tropicalis*			
Q6GND4	69.2	21	3	218.87	26	26	9653	Dbia protein	*Xenopus laevis*			
Q6AZL1	68.41	8	1	121.39	9	6	14,536	40S ribosomal protein S30	*Xenopus tropicalis*			
Q6AZK8	68.39	13	1	55.53	13	1	12,433	Novel protein similar to srp14	*Xenopus tropicalis*			
G5E3D7	66.04	8	1	50.66	8	1	14,261	Uncharacterized protein (Fragment)	*Hymenochirus curtipes*	ribonuclease UK114 [*Xenopus tropicalis*]	3.00E-84	NP_001265674.1
Q6P7M9	65.99	6	1	134.28	21	5	24,354	High-mobility group box 2	*Xenopus tropicalis*			
Q28FT1	61.57	10	2	157.71	21	10	21,726	Novel histone H1 family protein	*Xenopus tropicalis*			
Q28GJ3	60.22	8	1	53.01	8	1	14,637	Heat-responsive protein 12	*Xenopus tropicalis*			
Q90ZD7	54.2	12	2	194.87	21	12	22,546	Histone H1	*Bufo gargarizans*			
Q68F90	53.82	7	1	84.4	14	2	23,279	Nascent polypeptide-associated complex subunit alpha	*Xenopus tropicalis*			
Q6NVQ2	52.47	4	1	61.32	2	1	40,793	26S proteasome subunit	*Xenopus laevis*			
A5LHA4	52.25	3	1	47.81	4	1	38,519	Annexin	*Lithobates catesbeiana*			
Q9PWF7	49.37	1	1	166.76	17	12	60,251	Catalase	*Rugosa rugosa*			
F6X7G4	48.21	4	1	79.06	6	2	29,342	Cathepsin Z	*Xenopus tropicalis*			
C1C4P2	48.12	11	2	138.94	44	5	16,838	Calmodulin	*Lithobates catesbeiana*			
F6Y6U8	42.84	1	1	45.94	1	1	97,711	Uncharacterized protein	*Xenopus tropicalis*	calpastatin isoform X15 [*Xenopus tropicalis*]	0	XP_012811560.1
Q6NUH0	40.95	7	1	56.31	14	2	14,516	60S ribosomal protein L31	*Xenopus laevis*			
A9UMJ8	39.65	1	1	143.53	6	7	117,501	AP2-associated kinase 1	*Xenopus tropicalis*			

(*continued on next page*)

Table 4 (*continued*)

Accession	Analysis 1			Analysis 2			Average mass (Da)	Description	Organism	Blast alignment		
	-10lgP	Coverage (%)	Identified peptides	-10lgP	Coverage (%)	Identified peptides				Protein	*E*-value	Accession
F6QBI8	38.66	1	1	30.14	1	1	96,199	Cadherin 1 type 1	*Xenopus tropicalis*			
C1C3M2	37.59	3	1	54.82	6	2	35,412	NADP-dependent leukotriene B4 12-hydroxydehydrogenase	*Lithobates catesbeiana*			
Q28GR1	37.08	16	1	76.15	16	2	7072	Translation machinery-associated protein 7	*Xenopus tropicalis*			
Q9DGE5	34.88	2	1	65.6	6	3	39,439	Fructose-bisphosphate aldolase	*Xenopus laevis*			
A0A1L8H4S4	31.27	8	1	82.1	31	3	17,674	Uncharacterized protein	*Xenopus laevis*	60S ribosomal protein L23a [*Xenopus laevis*]	8.00*E*-108	XP_018101610.1
Q4H447	30.72	2	1	68.83	5	3	50,175	Elongation factor 1-alpha	*Xenopus tropicalis*			
B7ZPZ8	70,48	27	1	119.74	70	5	5097	Thymosin beta 4 peptide	*Xenopus laevis*			

3.3.2. Binding

We identified sixty-two binding proteins belonging to 15 different binding processes. Binding proteins might bind to several molecules (e.g., proteins, ions, fatty acids, lipids, etc.) and play important role in amphibian skin secretion.

3.3.2.1. Fatty-acyl-CoA binding. We found at least 2 acyl-coenzyme A binding proteins (ACBP) (also termed diazepam binding inhibitors, MGC116485 protein or Dbia protein) in *D. melanostictus* parotoid macrogland secretion, regardless of the batch processing. These proteins were already identified in *D. melanostictus* [22] and *B. gargarizans* [34] parotoid macrogland secretion.

ACBPs are 10 kDa cytosolic proteins, which bind with high affinity and specificity to medium and long-chain fatty acyl-CoA esters (C14 - C22) [35,36]. These soluble proteins can exert an important house-keeping role in lipid metabolism: I) protecting acyl-CoA esters from hydrolysis; II) extracting acyl-CoA esters from membranes; III) delivering acyl-CoA esters to phospholipid, glycerolipid and cholesterol ester and ceramide synthesis, to β-oxidation or fatty acid elongation [35]. Furthermore, proteolytically cleavage of ACBP can generate bioactive peptides capable of inhibiting diazepam binding to the GABA receptor [35,36].

3.3.2.2. Protein binding. Inside the granular glands, we found several granules localized in a central position of the gland. These granules vary in size and shape and exert a fundamental role: store a higher diversity of biological molecules [26,37,38]. Understanding the orign, organization and traffic of granules inside the gland would be very important and it is likely that several proteins could be involved in the process, such as:

3.3.2.2.1. Annexins. A conserved family of Ca^{2+}/lipid-binding proteins. This group has been implicated in the regulation of diverse cellular and physiological process, such as *endo-* and exocytosis, membrane/cytoskeleton interactions, membrane trafficking and scaffolding and vesicle organization [39–41]. Besides that, annexins can i) inhibit cytosolic phospholipase A2 [42], ii) interact with cathepsin B allowing selective degradation of extracellular matrix proteins and also, iii) block phosphatidylserine on the cell surface, which impact infectivity of *Toxoplasma* and *Leishmania* parasites [42,43].

3.3.2.2.2. Toll-interacting protein (Tollip). This protein presents 3 distinct domains: I) Tom1-binding domain (TBD): this domain is involved in protein sorting through Myb protein (TOM1), clathrin and ubiquitin interaction; II) Conserved 2 domain (C2): It binds to phospholipids in both a calcium-dependent and -independent manner, making possible Tollip localization with cellular membranes, such as cell membrane, endosome and lysosome; III) CUE domain: this domain is a ubiquitin-binding module, which interacts to ubiquitinated proteins. Furthermore, this domain is involved in protein sorting [44–48].

3.3.2.2.3. Histones. These nuclear proteins are normally associated to proper chromosome packing [49]. Histones can also exhibit antimicrobial activity: a) Seo et al. [50] isolated 3 antimicrobial histones H2B from *Crassostrea virginica* (American oyster); b) Jodoin & Hincke [51] described a novel antimicrobial property for histone H5 from chicken; c) Park et al. [52] described a potent antimicrobial peptide termed parasin I in *Parasilurus asotus* (wounded catfish) mucus; d) Buforin I (another histone H2A-derived antimicrobial peptide) was isolated from the stomach tissues of *Bufo gargarizans* [53].

3.3.2.3. Carbohydrate binding. Galectins are a conserved family of lectins that possess a carbohydrate recognition domain (CRD) responsible for β-galactoside binding. Gal-1 can also bind to proteins, such as actin, glycosaminoglycans or mucin [40,54]. They are involved in apoptosis, cell cycle and cell division and in the control of pre-mRNA splicing [55]. Furthermore, these innate immune proteins can bind to

Table 5
Proteins identified in C-BDF fraction.

Accession	Analysis 1			Analysis 2			Average mass (Da)	Description	Organism	Blast alignment		
	-10lgP	Coverage (%)	Identified peptides	-10lgP	Coverage (%)	Identified peptides				Protein	E-value	Acession
A4K520	359.4	65	15	272.07	72	31	9905	Diazepam binding inhibitor	*Bufo gargarizans*			
Q800P5	256.94	27	7	158.65	27	9	41,912	Beta actin (Fragment)	*Engystomops pustulosus*			
Q9PWF7	255.61	14	7	213.75	19	13	60,251	Catalase	*Rugosa rugosa*			
C1C4P2	242.94	44	8	144	39	6	16,838	Calmodulin	*Lithobates catesbeiana*			
P56217	232.28	33	10	189.1	42	16	14,711	Galectin-1	*Rhinella arenarum*			
Q7SY90	231.73	11	7	218.02	18	15	60,259	Catalase	*Xenopus laevis*			
Q6DFM4	226.6	25	7	134.64	25	8	29,016	Tropomyosin 1	*Xenopus tropicalis*			
G5DYL6	219.52	28	7	122.32	29	7	26,458	Putative tropomyosin 3 (Fragment)	*Hymenochirus curtipes*			
A0A1L8G6S1	213.84	25	6	131.16	33	7	26,318	Histone H4	*Xenopus laevis*			
C1C413	210.58	41	6	129.83	48	8	11,971	Pterin-4-alpha-carbinolamine dehydratase	*Lithobates catesbeiana*			
P45883	199.36	32	8	205.85	45	16	9808	Acyl-CoA-binding protein homolog	*Pelophylax ridibundus*			
Q4KLC5	197.54	36	7	139.11	47	8	8374	MGC116485 protein	*Xenopus laevis*	acyl-CoA-binding protein homolog [*Xenopus laevis*]	2.00*E*-43	XP_018124633.1
Q6GND4	192.8	24	3	109.49	24	2	9653	Dbia protein	*Xenopus laevis*			
A4K522	172.65	15	3	94.87	14	3	15,576	Superoxide dismutase [Cu−Zn]	*Bufo gargarizans*			
F7DNS3	168.44	7	4	77.86	4	3	72,704	Ubiquitin C	*Xenopus tropicalis*			
Q7ZYL1	159.05	20	3	61.45	4	1	26,635	Proteasome subunit beta type	*Xenopus laevis*			
Q4F8N6	158.92	32	5	66.25	27	3	14,968	Tropomyosin beta (Fragment)	*Dryophytes chrysoscelis*			
D5KU33	136.62	4	2	81.28	7	2	38,447	Annexin	*Bombina maxima*			
A4K523	133.07	12	2	57.66	7	1	22,339	Biliverdin reductase B	*Bufo gargarizans*			
F7C8E0	131.9	6	2	114.58	13	7	51,848	Coiled-coil domain-containing 6	*Xenopus tropicalis*			
Q6GL11	130.04	11	2	80.19	11	2	24,891	Charged multivesicular body protein 4b	*Xenopus tropicalis*			
F6TUH3	124.72	27	2	59.71	17	1	13,254	Myosin light chain 9	*Xenopus tropicalis*			
F6UZ27	124.53	3	1	61.47	2	1	72,496	Heat shock protein family A (Hsp70) member 5	*Xenopus tropicalis*			
A4K534	123.43	2	3	68.55	3	4	99,046	Uncharacterized protein	*Bufo gargarizans*	TRPM8 channel-associated factor homolog [*Nanorana parkeri*]	0	XP_018419924.1
A0A1L8GFL4	122.96	6	3	80.1	6	2	37,238	Uncharacterized protein	*Xenopus laevis*	alcohol dehydrogenase [NADP(+)]-like [*Xenopus laevis*]	0	XP_018116320.1
F6UFZ4	122.08	11	1	84.01	11	3	13,202	Glutathione peroxidase 3	*Xenopus tropicalis*			
F7DY42	121.62	10	2	81.34	18	3	27,298	Tyrosine 3-monooxygenase/ tryptophan 5-monooxygenase activation protein epsilon	*Xenopus tropicalis*			
Q5XGB0	119.59	8	2	74.41	10	2	35,938	Aldo-keto reductase family 1 member B7	*Xenopus tropicalis*			
Q28IY4	110.87	6	2	80.42	6	2	40,360	Adenosine kinase	*Xenopus tropicalis*			
A0A1L8I1Z7	110.65	5	2	90.08	7	4	63,065	Beta-hexosaminidase	*Xenopus laevis*			
C1C3W4	108.89	11	2	95.39	22	5	9994	Acyl-CoA-binding protein	*Lithobates catesbeiana*			
Q90ZD8	106.34	22	2	46.45	7	1	13,973	Histone H2A	*Bufo gargarizans*			
F7C2U5	105.2	12	2	88.73	11	3	22,676	Insulin like growth factor binding protein 5	*Xenopus tropicalis*			

(*continued on next page*)

Table 5 (*continued*)

Accession	Analysis 1			Analysis 2			Average mass (Da)	Description	Organism	Blast alignment		
	-10lgP	Coverage (%)	Identified peptides	-10lgP	Coverage (%)	Identified peptides				Protein	E-value	Acession
Q6DEY4	99.1	5	2	66.63	5	2	68,901	Eukaryotic translation initiation factor 4B	*Xenopus tropicalis*			
Q5M8L9	98.3	9	2	78.18	9	3	23,444	EF-hand domain family member D2	*Xenopus tropicalis*			
Q28FW1	97.62	4	1	73.52	4	2	30,122	Inositol-1-monophosphatase	*Xenopus tropicalis*			
Q642N4	97.02	6	2	79.93	6	3	35,907	Ltb4dh protein	*Xenopus tropicalis*			
B7ZU10	90.73	6	2	98.7	11	5	35,995	Uncharacterized protein	*Xenopus tropicalis*	prostaglandin reductase 1 [*Xenopus tropicalis*]	0	
Q66IY5	90.55	9	2	51.1	5	1	24,542	MGC84072 protein	*Xenopus laevis*	brain abundant membrane attached signal protein 1 S homeolog [*Xenopus laevis*]	1.00E-153	NP_001087724.1
Q6DF14	88.46	4	1	30.18	2	1	31,994	Thioredoxin-like 1	*Xenopus tropicalis*			
A0A1L8HLJ7	87.57	2	1	84.75	7	3	49,713	Uncharacterized protein	*Xenopus laevis*	testican-3-like [*Xenopus laevis*]		
F6 U247	84.59	2	1	47.91	2	1	54,978	Tubulointerstitial nephritis antigen-like 1	*Xenopus tropicalis*		0	
Q6DFT7	68.55	4	1	76.9	6	2	38,185	Phyh-prov protein	*Xenopus laevis*			
Q9W6D4	67.64	3	1	47.8	3	1	42,855	Cathepsin D	*Hynobius leechii*			
Q640H5	64.72	3	1	43.55	2	1	46,849	Isocitrate dehydrogenase [NADP]	*Xenopus laevis*			
C1C3Q9	59.01	5	1	46.41	10	1	16,987	Ubiquitin-conjugating enzyme E2 L3	*Lithobates catesbeiana*			
Q3KQ87	57.23	3	1	43.33	3	1	46,402	MGC130872 protein	*Xenopus laevis*	galactosidase alpha S homeolog precursor [*Xenopus laevis*]	0	NP_001089687.1
Q6P382	57.16	9	1	66.53	9	1	12,361	Eukaryotic translation initiation factor 4E binding protein 2	*Xenopus tropicalis*			
A0A1W6BSK9	55.31	10	1	60.99	10	1	9913	Myosin light polypeptide 6 (Fragment)	*Plethodon dunni*			
Q6DFR0	55.28	5	1	76.98	6	2	30,069	Toll-interacting protein	*Xenopus tropicalis*			

Table 6
Proteins identified in AC-SDF fraction.

Accession	Analysis 1			Analysis 2			Average mass (Da)	Description	Organism	Blast alignment		
	-10lgP	Coverage (%)	Identified peptides	-10lgP	Coverage (%)	Identified peptides				Protein	E-value	Acession
F7DNS3	202.61	6	4	161.68	85	11	72,704	Ubiquitin C[a]	*Xenopus tropicalis*			
A9UMJ8	170.31	1	3	111.84	3	3	117,501	AP2-associated kinase 1	*Xenopus tropicalis*			
A4K520	165.02	41	3	140.33	47	5	9905	Diazepam binding inhibitor	*Bufo gargarizans*			
A0A0U3A3X0	154.76	7	3	150.42	20	8	41,882	Gamma actin	*Bufo gargarizans*			
Q5XGB4	124.8	5	2	60.17	12	2	24,921	Brain abundant membrane attached signal protein 1	*Xenopus tropicalis*			
P56217	117.48	21	3	105.18	16	4	14,711	Galectin-1	*Rhinella arenarum*			
A0A1L8G6S1	113.17	8	2	110.85	18	6	26,318	Histone H4	*Xenopus tropicalis*			
Q6NVM0	107.74	10	2	69.36	11	2	21,006	Histone H1.0	*Xenopus tropicalis*			
Q5M8E1	104.95	5	1	72.43	9	2	24,601	Peroxiredoxin 6	*Xenopus tropicalis*			
A4K522	104.87	14	2	56.48	7	1	15,576	Superoxide dismutase [Cu−Zn]	*Bufo gargarizans*			
G5E3D7	103.88	8	1	56.74	8	1	14,261	Uncharacterized protein (Fragment)	*Hymenochirus curtipes*	ribonuclease UK114 [*Xenopus tropicalis*]	3.00E-84	NP_001265674.1
P08776	86.96	2	1	132.01	10	7	55,679	Keratin type II cytoskeletal 8[a]	*Xenopus laevis*			
Q6DJ70	84.16	7	1	100.84	13	3	16,122	Hemoglobin subunit gamma 2[a]	*Xenopus tropicalis*			
Q0VGV3	78.83	30	2	101.24	51	4	7838	Ribosomal protein S28 pseudogene 9[a]	*Xenopus tropicalis*			
Q28GJ3	76.61	8	1	56.15	8	1	14,637	Heat-responsive protein 12	*Xenopus tropicalis*			
F6SVX8	76.49	4	1	49.73	4	1	35,649	Eukaryotic translation initiation factor 3 subunit G[a]	*Xenopus tropicalis*			
Q9I9P5	68.57	2	1	146.7	11	9	56,619	Inner-ear cytokeratin[a]	*Lithobates catesbeiana*			
Q6NWX0	67.78	2	1	59.19	6	2	56,249	ATP synthase subunit beta[a]	*Xenopus tropicalis*			
Q90ZD6	64.61	7	1	63.28	18	2	13,816	Histone H2A	*Bufo gargarizans*			
Q5BKM5	63.74	2	1	66.77	3	2	44,167	RAD23 homolog B nucleotide excision repair protein[a]	*Xenopus tropicalis*			
Q6P382	61.08	9	1	73.64	12	1	12,361	Eukaryotic translation initiation factor 4E binding protein 2[a]	*Xenopus tropicalis*			
D5KU33	48.39	3	1	40.89	4	1	38,447	Annexin	*Bombina maxima*			
Q7ZYU6	45.93	4	1	72.99	4	2	28,807	MGC52685 protein[a]	*Xenopus laevis*	carbonic anhydrase 2 S homeolog [*Xenopus laevis*]	0	NP_001079371.1

[a] Proteins only identified after subsequent anionic and cationic batch processing.

Table 7
Proteins identified in AC-BDF fraction.

Accession	Analysis 1			Analysis 2			Average mass (Da)	Description	Organism	Blast alignment		
	-10lgP	Coverage (%)	Identified peptides	-10lgP	Coverage (%)	Identified peptides				Protein	E-value	Accession
A7J0U5	139.1	30	3	63.8	10	1	14,742	Ubiquitin/ribosomal protein L40 fusion protein[a]	*Bufo gargarizans*			
A9JSP7	133.83	8	3	86.76	6	2	16,000	Hemoglobin epsilon 1[a]	*Xenopus tropicalis*			
I6ZFH6	109.19	5	2	94.89	5	2	42,839	Keratin 5 (Fragment)[a]	*Ambystoma mexicanum*			
C1C4Q1	99.06	9	2	52.61	4	1	27,387	Proteasome subunit alpha type	*Lithobates catesbeiana*			
A4K520	89.15	24	2	57.16	16	1	9905	Diazepam binding inhibitor	*Bufo gargarizans*			
Q9PWF7	85.46	3	2	112.65	11	4	60,251	Catalase	*Rugosa rugosa*			
B7ZU10	74.55	3	1	48.68	4	1	35,995	Uncharacterized protein	*Xenopus tropicalis*	prostaglandin reductase, isoform X1 [*Xenopus tropicalis*]	0	XP_017953051.1
D5KU33	73.82	3	1	70.11	4	2	38,447	Annexin	*Bombina maxima*			
A4K534	70.86	2	1	72.95	2	1	99,046	Uncharacterized protein	*Bufo gargarizans*	TRPM8 channel-associated factor homolog [*Nanorana parkeri*]	0	XP_018419924.1
A0A0U3A3X0	64.44	4	1	79.35	7	2	41,882	Gamma actin	*Bufo gargarizans*			
B1H2Y5	56.16	2	1	44.37	2	1	31,767	BCL2-like 14 (apoptosis facilitator)[a]	*Xenopus tropicalis*			

[a] Proteins only identified after subsequent anionic and cationic batch processing.

and agglutinate bacteria, and even more to kill bacteria directly, being not necessary the activation of other factors [55,56]. Galectins have already been identified in *R. schneideri* parotoid macrogland secretion [19].

3.3.2.4. Endoplasmic reticulum signal peptide binding. We identified a protein termed novel protein similar to srp14. The signal recognition particle (SRP) is a ribonucleoprotein complex involved in targeting secretory proteins to the endoplasmic reticulum (ER) membrane in eukaryotes. During protein synthesis in the ribosome, SRP can recognize a signal sequence present in the nascent chain and in associations with other proteins, the nascent chain is target to ER [57].

3.3.2.5. Organic cyclic compound binding. Amphibians are constantly exposed to ultraviolet radiation (UV), which can cause protein denaturation, even though DNA damage [27–29]. We identified two proteins involved in i) protection against UV radiation damage and ii) protein recycling.

3.3.2.5.1. Heat shock proteins (HSPs). Under environmental or physiological stresses, synthetized HSPs interact with denatured proteins and help them to i) refold and reassemble, turning back their active forms, and ii) avoid protein aggregation. Once this system repairs fail, HSP70, for example, can interact with co-chaperone HSP40 and facilitate damaged protein degradation through the ubiquitin-proteasome pathway [58]. HSPs can also help to fold newly synthesized peptides or assemble protein complexes and assist in membrane translocation of organellar and secretory proteins [59,60].

3.3.2.5.2. RAD23 homolog B, nucleotide excision repair protein. This protein has four domains: i) one Rad4-binding domain, ii) one N-terminal ubiquitin-like (UbL) domain and iii) two ubiquitin-associated domains (UBA). The first one forms a complex with others Rad proteins and participates in the nucleotide excision repair induced by UV radiation damage on DNA. Furthermore, UBA domains can bind to mono- and polyubiquitylated proteins and direct them to proteasome degradation through interaction between UbL domain and Rpn1 subunit of 19S proteasome. Rad23 is released after to resist against proteasome degradation [61].

3.3.2.6. Ion binding. Calmodulin is a Ca^{+2} binding protein that regulates some pathophysiological roles, such as apoptosis, inflammation and smooth muscle contraction. This regulation occurs via calcium-dependent modulation of different enzyme activities (phosphatases and protein kinases) or signaling proteins (channels and structural proteins and membrane receptors) [62]. Due to these activities, calmodulin participates in the immune response [63]. Cavalcante et al. [33] identified calmodulin-binding motifs in the venomic analysis of *D. muelleri* skin secretion.

3.3.3. Catalytic activity

Libério et al. [64] described the presence of peptidases (dipeptidyl peptidases (DPPs) and metallopeptidases) in *Leptodactylus labyrinthicus* skin secretion. According to the authors, these enzymes may be involved in tegument homeostasis and in peptide processing. Recently, Souza et al. [65] identified and characterized a phospholipase A2 enzyme from the anuran skin secretion *Pithecopus azureus*.

Cavalcante et al. [33] reported the presence of both metallo and serine-peptidases in *D. muelleri* skin secretion, at the biochemical and proteomic level. These authors commented that in *D. muelleri*, an amphibian that does not secrete peptides in its skin secretion, the healthiness of the skin ought to be ensured by other molecular groups.

Here, we describe not only the presence of peptidases (including proteasome subunits), but also the presence of kinases, reductases and peroxidases among others. All enzymes involved in the redox balance were discussed in section 3.3.1.

3.3.3.1. Hydrolase activity

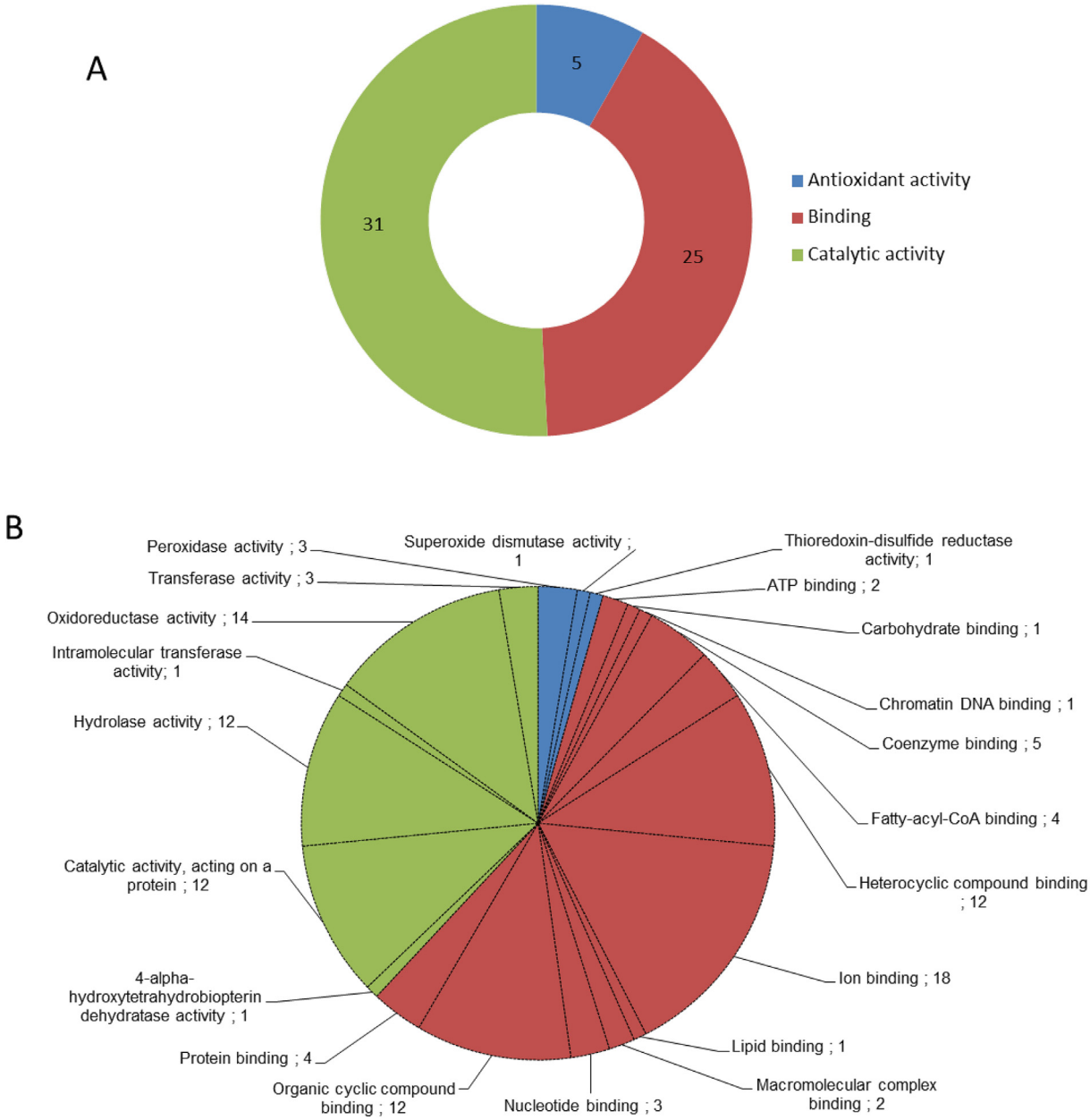

Fig. 1. A–D Proteins were classified according to GO Project. All proteins identified in both A-SDF and A-ADF fractions were classified according to its (A; C) molecular function and (B; D) molecular function sub-categories, respectively.

3.3.3.1.1. Proteasome (EC 3.4.25.1). Proteasomes are the second most abundant cellular protein complexes (up to 5% of the total proteins) and a key protease responsible for the ubiquitin-dependent protein degradation [66]. The proteasome holoenzyme is composed by a proteolytic core particle (CP or 20S proteasome) and a regulatory particle (RP, 19S proteasome). The configuration RP–CP is referred as 26S proteasome [67]. This complex plays crucial roles in cellular processes, such as gene expression, regulation of cell cycle progression, transcription and the quality control of newly synthesized proteins [66,67]. Cellular protein degradation occurs via ubiquitin-proteasome system in eukaryotic cells. Initially, proteins were marked by the addiction of a ubiquitin chain molecule. Then, they are degraded by 26S proteasome in the cytoplasm or nucleus. Other proteins may be involved in this process, such as ubiquitins, chaperones, HSP and RAD23 [66,67].

3.3.3.1.2. Fumarylacetoacetate hydrolase domain-containing protein 2 (FAH2). Fumarylacetoacetate hydrolase (FAH), a member of FAH superfamily, participates during the degradation pathway of tyrosine and phenylalanine in mammals. Located in the cytosol, FAH catalyzes the hydrolysis of 4-fumarylacetoacetate into acetoacetate and fumarate, both products metabolized in biosynthetic or energetic pathways. There is little information about FAH2 protein on the literature [68].

3.3.3.1.3. Cathepsins. This protease group comprises different catalytic enzymes involved in protein turnover within the lysosome [69].

The aspartic endopeptidase cathepsin D (EC 3.4.23.5) is synthetized at rough endoplasmatic reticulum as a proenzyme. Once its signal peptide is removed, this protein is target to intracellular vesicular structures (lysosomes, endosomes, phagosomes), where it become active after specific cleavages [70]. Beyond to protein turnover, cathepsin D is related to i) activation and degradation of polypeptide hormones chemokines, growth factors and their receptors, like FGF [71] and endotastin [72]: ii) activation of enzymatic precursors, such as cathepsin B [73] and cathepsin L [74] and iii) degradation of cytoskeletal proteins

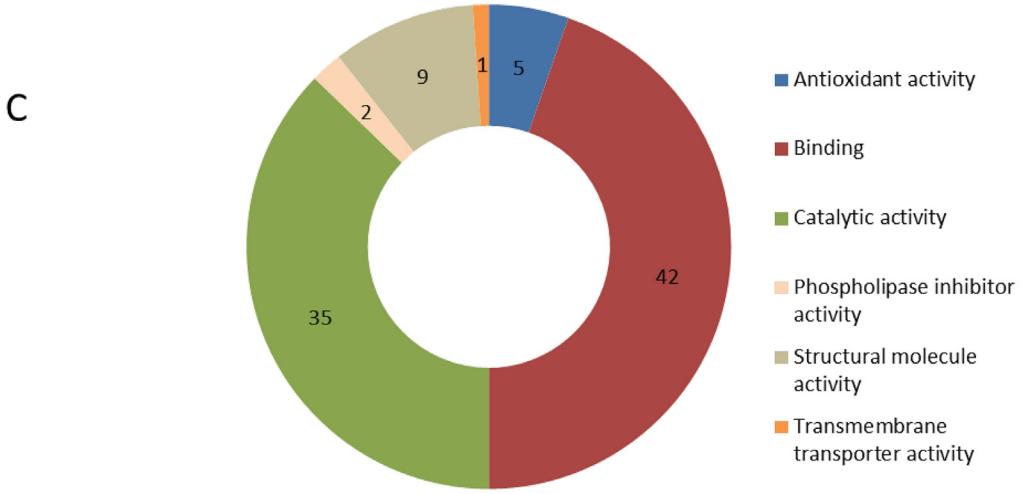

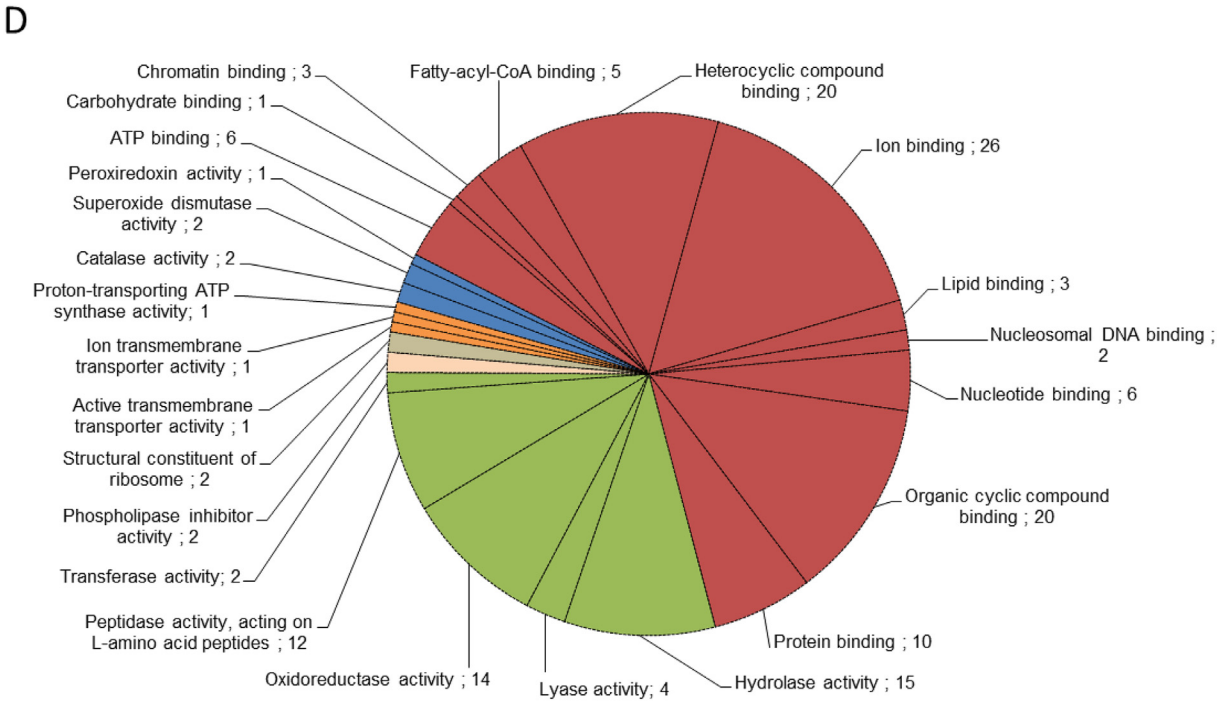

Fig. 1. (*continued*)

[70,75].

The cysteine exopeptidase cathepsin X (or Z) (EC 3.4.18.1) is expressed in immune system cells in humans, such as monocytes, macrophages and dendritic cells. This suggests the involvement of this enzyme in immune response regulation and phagocytosis [76]. Cathepsin X is activated by transprocessing by cathepsin L or S. This process involves the cleavage of cathepsin X in a residue situated at the junction of prodomain and the mature domain [77].

We identified cathepsins D and X in our study (Tables 2, 4–5), as well as cathepsins B, C, L and V (supplemental material 2).

3.3.3.1.4. Glycosidases. Alpha-galactosidase (EC 3.2.1.22) catalyzes the removal of a terminal α-galactose residue from polysaccharides, glycolipids, and glycopeptides in the lysosomes [78]. Beta-hexosaminidase (E.C. 3.2.1.52), another lysosomal enzyme, catalyze the hydrolysis of terminal non-reducing *N*-acetyl-d-hexosamine residues in *N*-acetyl-β-d-hexosaminide [79].

3.3.3.1.5. Inositol-1-monophosphatase (EC 3.1.3.25). This is a key enzyme in the inositol recycling. It catalyzes the dephosphorylation of inositol monophosphates to produce free inositol [80]. Free inositol can be used to synthesize phosphoinositides, which interact with other proteins and participate in diverse cellular process, such as cytoskeleton remodeling, membrane traffic and ion channel regulation [81].

3.3.3.1.6. A disintegrin and metalloproteinase with thrombospondin motifs 15-like (ADAMTS-15) (EC: 3.4.24.-). The ADAMTS family comprises 19 secreted proteases in humans, involved in cleavage of extracellular matrix (ECM) proteoglycans, collagen matrix assembly and vascular hemostasis. This protein family has a compound domain structures that consist of: pro-region; metalloproteinase and disintegrin-

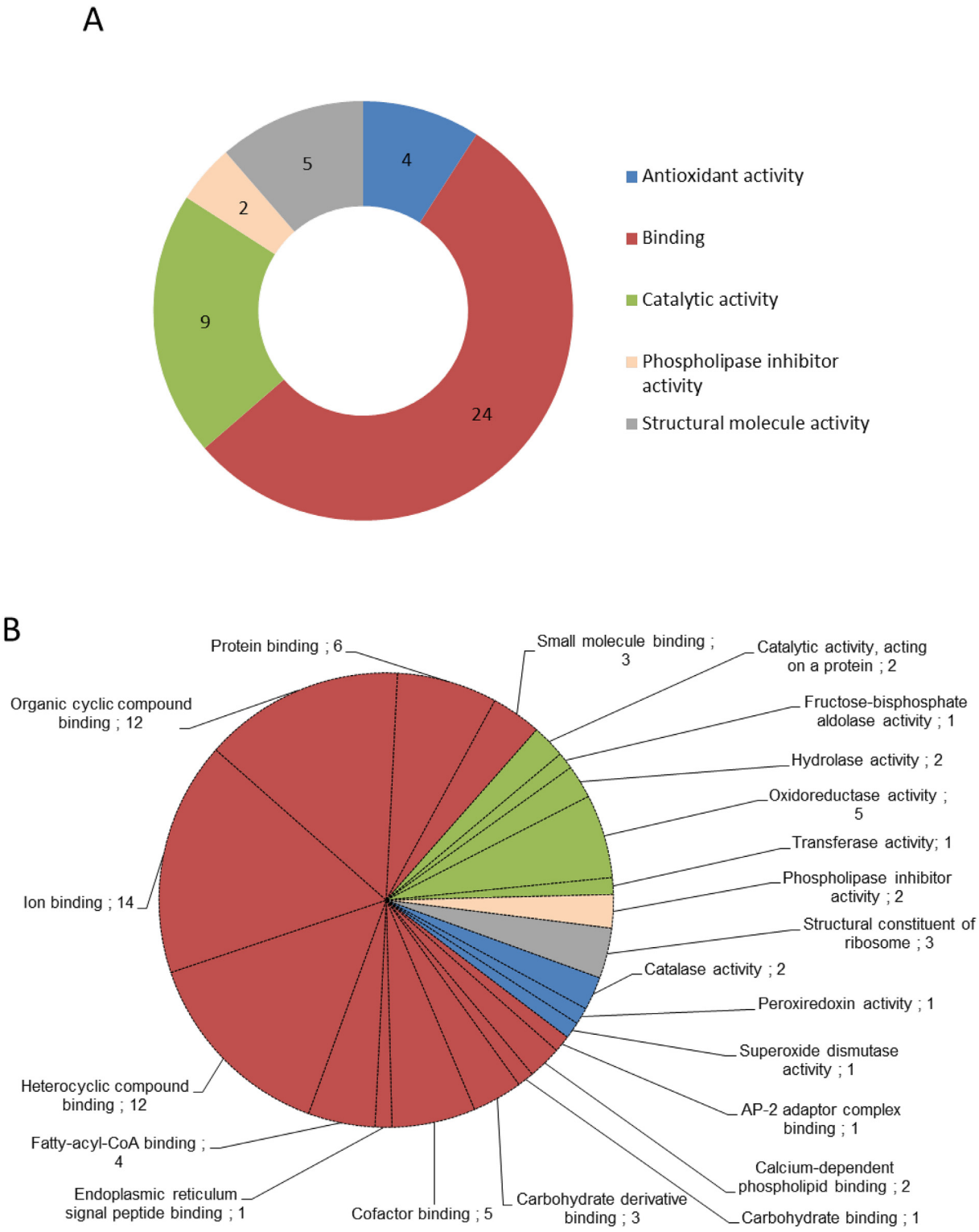

Fig. 2. A–D Proteins were classified according to GO Project. All proteins identified in both C-SDF and C-BDF fraction were classified according to its (A; C) molecular function and (B; D) molecular function sub-categories, respectively.

like domains; a central thrombospondin type I repeat (TSR); a cysteine-rich stretch; and a spacer region, followed by a variable number of TSRs and additional modules, which vary according to the family member [82]. ADAMTS15 belongs to the aggrecanase and proteoglycanase clades, hydrolases capable to cleave hyaluronan-binding chondroitin sulfate proteoglycan (CSPG) extracellular proteins, including aggrecan, brevican, neurocan and versican [82]. Besides, through its TSR domain, ADAMTS15 can be involved in the generation of cryptic anti-angiogenic peptides [83].

Regarding the toxin role of the peptidases, there has been a *Toxins* (ISSN 2072–6651) issue dealing specifically with the subject. In that volume, authors describe peptidases triggering pro-inflammatory responses [84], pro-coagulant activities [85] and insecticide enzymes [86], among others.

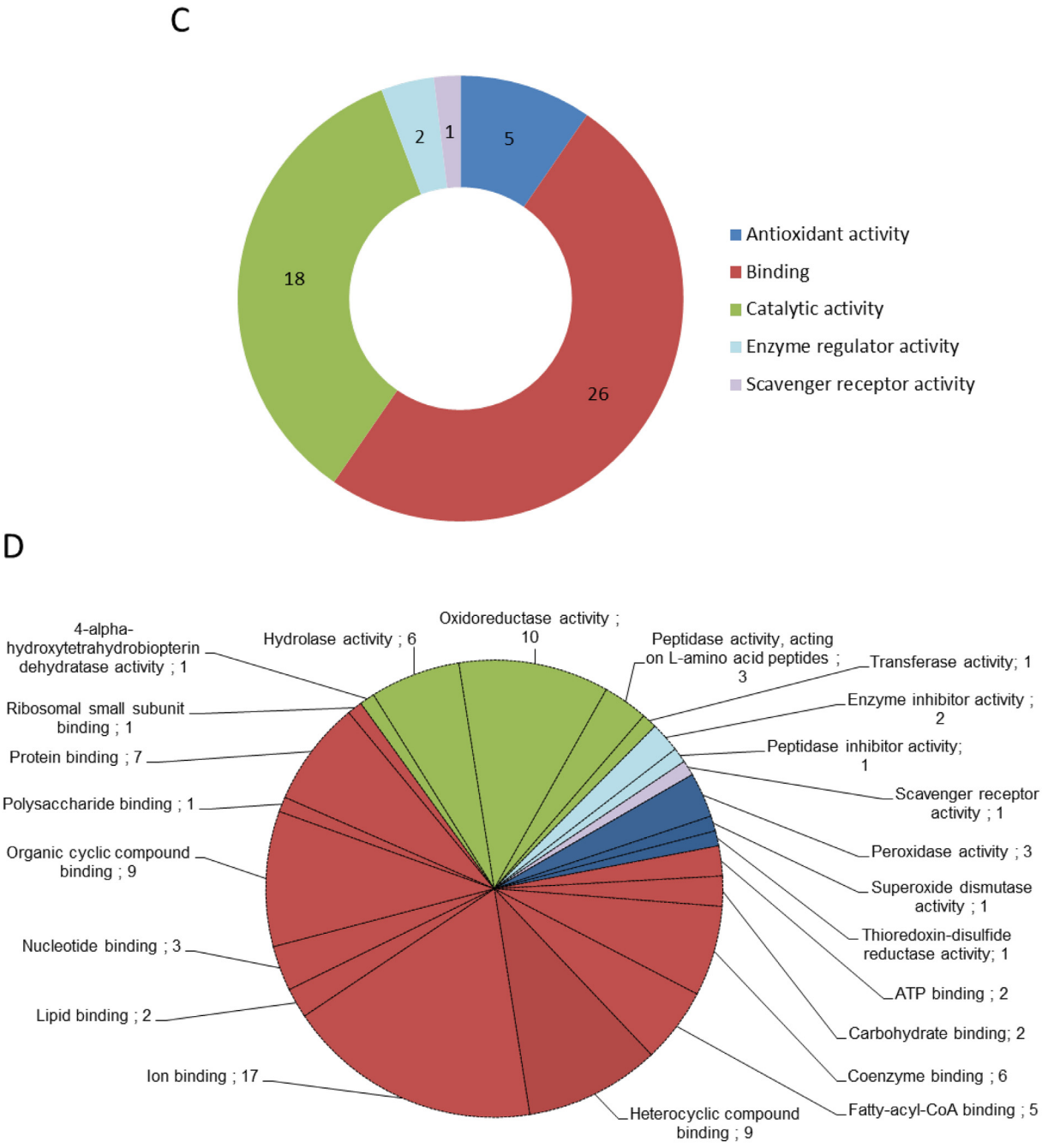

Fig. 2. (*continued*)

Normally, anurans display a passive defense against predators. The augmentation of the low molecular-mass chemical weaponry by toxic peptidases would enhance the defense strategies. Moreover, since no classical bioactive peptide has ever been described for bufonids, including the present work, such peptidases might be responsible for in situ cryptides generation [87], in response to given aggressions.

Fish cryptides were described as being toxic molecules [88]. Snakes also present cryptides in their venom [89]. Both classes are phylogenetically related to Amphibia class. Our data show the presence of some peptidase and proteins (histones, ACBP) already described as possible source of bioactive peptides. Besides, cathepsins B, D and L can cleave proteins and generate biological active peptides/proteins [71,72,90]. However, this hypothesis must be further studied.

Table 8 summarizes others proteins classified as “catalytic activity” in our study.

3.3.4. Others proteins

Here, we present all proteins classified based on molecular function, according to GO Project. However, some of them do not possess any classification, so far, as presented in Table 8. Furthermore, we would like to highlight two proteins: TRPM8 channel-associated factor homolog (recently identified in *B. gargarizans* [34] and charged multivesicular body protein 4b.

3.3.4.1. TRPM8 channel-associated factor homolog. TRPM8 is a homotetrameric, nonselective cation channel that is active by cold or by compounds inducing cooling sensation [91]. Gkika et al. [92] identified two proteins called TRP channel–associated factors (1 and 2) (TCAFs) in healthy mouse prostates that binds to TRPM8 and promote its trafficking to the cell surface. TCAF 1 show a higher similarity with TRPM8 channel-associated factor homolog from

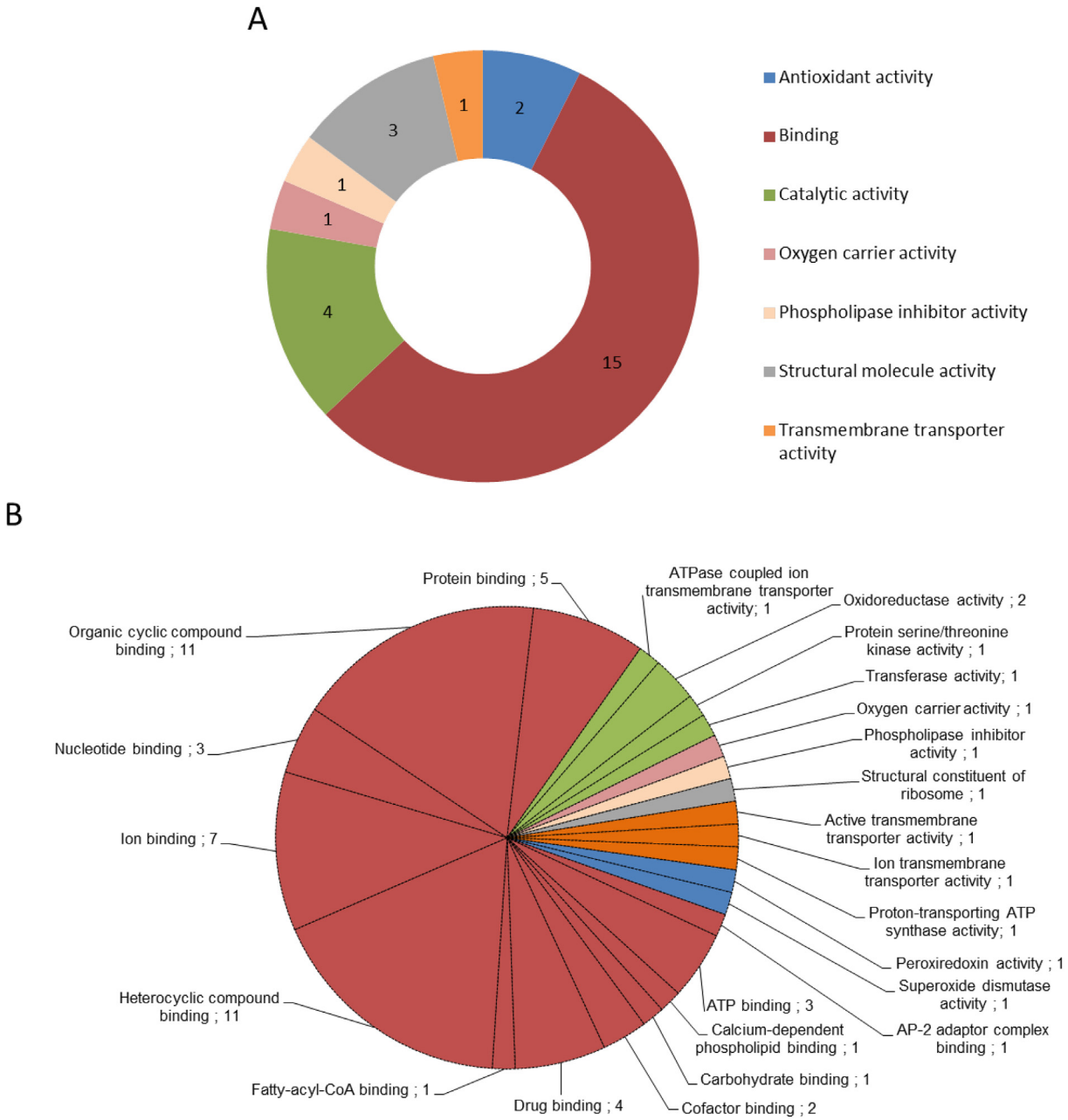

Fig. 3. A–D Proteins were classified according to GO Project. All proteins identified in both AC-SDF and AC-BDF fractions were classified according to its (A; C) molecular function and (B; D) molecular function sub-categories, respectively.

Nanorana parkeri (query coverage: 99%, identity 45%, *E*-value 0). TRPM8 channel-associated factor has a peptidase M60 domain (Pfam 13,402), which contains a zinc metallopeptidase motif (HEXXHX(8,28) E) and exhibit mucinase activity [93]. Tapader et al. [94] studied the protein YghJ, a cell surface associated and secreted lipoprotein containing a peptidase M60 domain from *Escherichia coli*. The authors showed that YghJ cause extensive hemorrhage in mouse ileum, attributing to the metalloprotease domain the hemorrhagic damage observed.

3.3.4.2. Charged multivesicular body protein 4b. This protein is a probable core component of the endosomal sorting required for transport complex III (ESCRT-III). This complex is involved in multivesicular bodies (MVBs) formation and sorting of endosomal cargo proteins into MVBs. It is believed that the complex ESCRT-III mediates the necessary vesicle extrusion and/or membrane fission activities, possibly in conjunction with other proteins (Uniprot function - Q9H444).

3.4. Hydrolase activity

Fig. 4 shows the biological activity retrieval assay of all fractions by zymography. It is possible to observe the presence of a prominent hydrolase activity in A-SDF and C-SDF (Fig. 4, line 1 and 2, respectively). Besides that, AC-SDF and C-BDF fractions showed a discrete biological activity at higher molecular mass (Fig. 4, line 3 and 4, respectively). These results reinforce our proteomic data. Furthermore, it is in agreement with the biological activity results observed by Mariano et al. [21] in *D. melanostictus* parotoid macrogland secretion. Moreover, both anionic and cationic batch sample preparation were efficient to retrieve proteins retaining their biological activities.

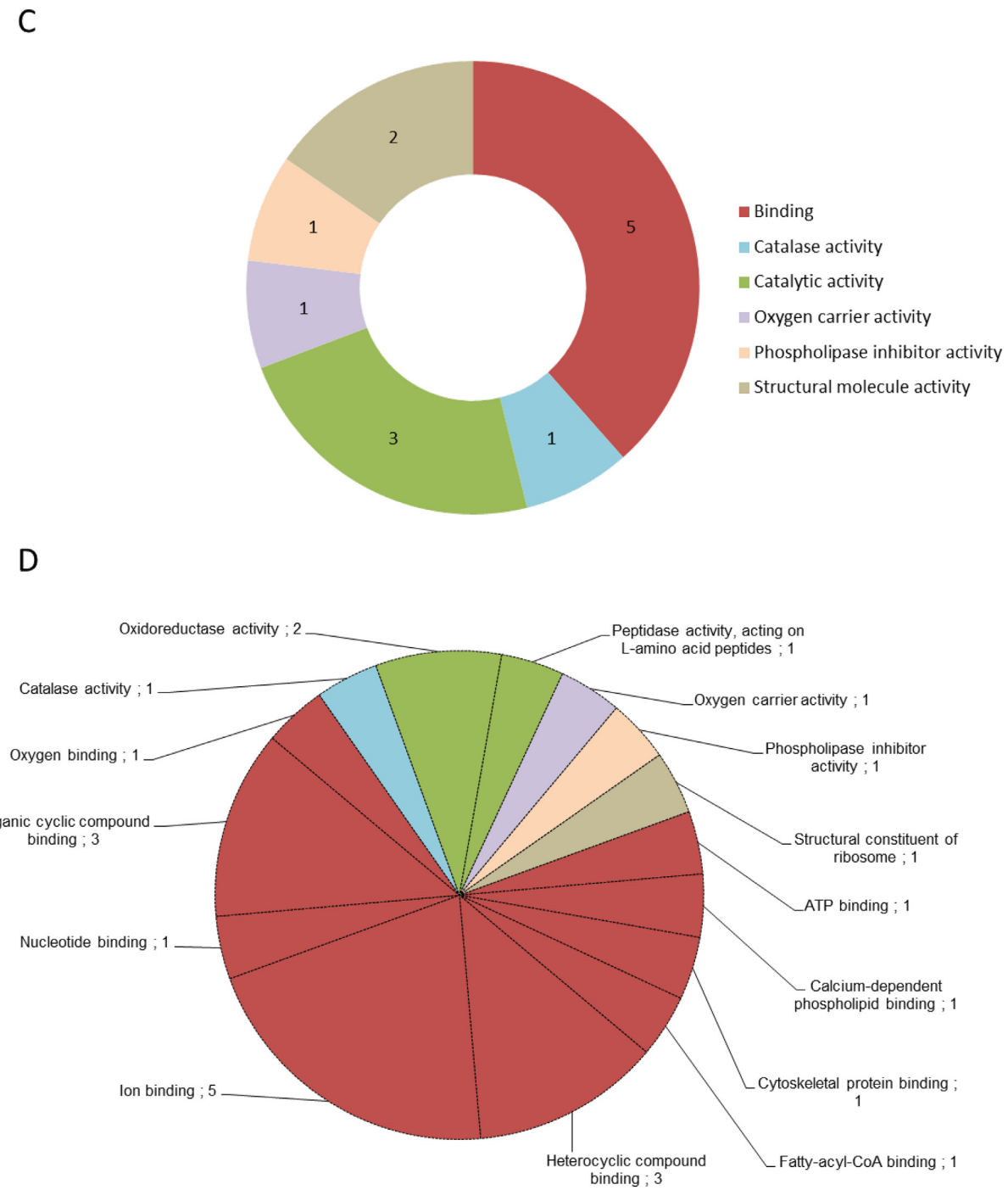

Fig. 3. (*continued*)

4. Conclusion

Sample preparation is crucial to any biological study. Recently, we described an IEx batch sample preparation [21], in which soluble proteins were retrieved from a viscous matrix (*D. melanostictus* parotoid macrogland secretion). In the present work, by using the batch methodology (anionic ion exchange) in association to a new batch sample preparation variation (cationic ion exchange), we successfully identified several proteins not yet described in bufonids parotoid macrogland secretion.

Independently of the batch methodology (anionic or cationic IEx), both were efficient to retrieve proteins from a viscous matrix as well as maintaining the assayed biological activity (peptidasic). Besides that, cationic batch processing in A-UB retrieved some proteins retained in the unbounded fraction, which certainly contributed to the overall proteomic interpretation.

Here, we report proteins related to energy metabolism, homeostasis, lipid metabolism, lipid/protein binding and membrane trafficking. All these housekeeping proteins surely contribute to the gland homeostasis. Moreover, the bufonid parotoid gland in syncytial, i.e., upon mechanical compression not only the venom, but also all the cellular contents – including organelles - are expelled. Any 1D SDS-PAGE analysis reveals the presence of many proteins in the venom, but the question regarding their role in the secretion remained unknown, mainly because the physicochemical characteristic of the venom impaired proper proteomic analyses. The present work performed a thorough analysis of the

Table 8
Others identified proteins and their biological process/molecular function in *D. melanostictus* parotoid macrogland secretion.

Gene ontology		Protein	Acession	Gene ontology classification
Catalytic activity	Hydrolase activity	AP2-associated kinase 1	A9UMJ8	positive regulation of Notch signaling pathway; protein phosphorylation; regulation of clathrin-dependent endocytosis *
		ATP synthase subunit beta	F7CIH4	ATP synthesis coupled proton transport *
	Intramolecular transferase activity	Phosphoglucomutase 1	Q6NVJ0	carbohydrate metabolic process *
	Lyase activity	Carbonic anhydrase 2 S homeolog	NP_001079371.1	carbonate dehydratase activity; zinc ion binding #
		Fructose-bisphosphate aldolase	Q9DGE5	glycolytic process *
		Pterin-4-alpha-carbinolamine dehydratase	C1C413	tetrahydrobiopterin biosynthetic process *
	Oxidoreductase activity	Alcohol dehydrogenase [NADP(+)]-like	XP_018116320.1	oxidoreductase activity #
		Aldo-keto reductase	Q5XGB0	oxidoreductase activity #
		Isocitrate dehydrogenase [NADP]	Q640H5	isocitrate metabolic process; tricarboxylic acid cycle *
		L-lactate dehydrogenase	Q6P7L5	carbohydrate metabolic process; carboxylic acid metabolic process *
		Malic enzyme	A0A1L8G977	malate dehydrogenase (decarboxylating) (NAD+) activity; metal ion binding; NAD binding #
		NADP-dependent leukotriene B4 12-hydroxydehydrogenase (Ltb4; prostaglandin reductase 1)	C1C3M2	15-oxoprostaglandin 13-oxidase activity; 2-alkenal reductase [NAD(P)] activity #
		Quinoid dihydropteridine reductase S	NP_001089804.1	oxidoreductase activity #
	Transferase activity	Adenosine kinase	Q28IY4	purine ribonucleoside salvage *
		Elongation factor 1-alpha	Q4H447	GTPase activity; GTP binding; translation elongation factor activity #
		Transaldolase	C1C4S1	carbohydrate metabolic process; pentose-phosphate shunt *
		Ubiquitin-conjugating enzyme E2 L3	C1C3Q9	ATP binding; transferase activity #
Other proteins		Biliverdin reductase B	A4K523	unclassified protein
		Calpastatin	XP_012811560.1	unclassified protein
		Nascent polypeptide-associated complex subunit alpha	Q68F90	transport #
		Phytanoyl-CoA dioxygenase, peroxisomal-like	XP_018108213.1	unclassified protein
		Testican-3-like	XP_018098712.1	calcium ion binding *
		Ubiquitin C	F7DNS3	unclassified protein

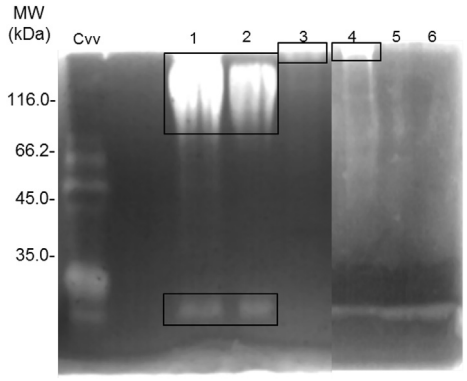

Fig. 4. Zymograms: Biological activity retrieval assays of (1) A-SDF, (2) C-SDF, (3) AC-SDF, (4) C-BDF, (5) A-ADF, (6) AC-BDF. All samples were lyophilized, resuspended in water and submitted to a 12% SDS-PAGE gel copolymerized with casein. *Crotalus viridis viridis* (cvv) (10 ng) was used as positive control. The boxes indicate the biological activity, for better visualization. Gel images were digitally composed for better visualization.

IEX-extracted proteins aiming to classify (and not quantify) them, by employing a broad GO keyword grouping.

Although no evident toxic protein was identified, it is important to mention that bufonids secretions are rich in alkaloids and steroids to which many toxic effects have already been associated. As a consequence, some of the identified proteins could be linked to these molecules' synthesis/transport and their presence in the venom could a consequence of a devoted cellular apparatus that has evolved in these glands for the benefit of the synthesis and storage of the low molecular mass molecules that, ultimately, would be the actual venom.

In conclusion, this work may increase the knowledge about amphibian granular gland/parotoid macrogland secretion, a major gland involved in the anuran chemical defense.

Funding

This work was funded by Coordenação de Aperfeiçoamento de Pessoal de Nível Superior (CAPES, DOCM grant 969130), Conselho Nacional de Desenvolvimento Científico e Tecnológico (CNPq, DCP grant 406385/2018-1) and São Paulo Research Foundation (FAPESP) / GlaxoSmithKline (Grant 2015/50040-4). DCP is a CNPq fellow researcher (Grant 303792/2016-7).

Appendix A. Supplementary data

Supplementary data to this article can be found online at https://doi.org/10.1016/j.jprot.2019.103525.

References

[1] C.R. Tracy, K.A. Christian, C.R. Tracy, Not just small, wet, and cold: effects of body size and skin resistance on thermoregulation and arboreality of frogs, Ecology 91 (2010) 1477–1484.
[2] E.H. Larsen, H. Ramløv, Role of cutaneous surface fluid in frog osmoregulation, Comp. Biochem. Physiol. A Mol. Integr. Physiol. 165 (2013) 365–370, https://doi.org/10.1016/j.cbpa.2013.04.005.
[3] R.C. Toledo, C. Jared, Cutaneous granular glands and amphibian venoms, Comp. Biochem. Physiol. A. 111 (1995) 1–29, https://doi.org/10.1016/0300-9629(95)98515-I.
[4] V. Erspamer, E.G. Falconieri, J.M. Cei, Active peptides in the skins of two hundred and thirty American amphibian species, Comp. Biochem. Physiol. C 85 (1986) 125–137.
[5] J.W. Daly, The chemistry of poisons in amphibian skin, Proc. Natl. Acad. Sci. U. S. A. 92 (1995) 9–13.
[6] E.D. Jr Brodie, P.K. Ducey, E.A. Baness, Antipredator skin secretions of some tropical salamanders (Bolitoglossa) are toxic to snake predators, Biotropica 23 (1991) 58–62, https://doi.org/10.2307/2388688.
[7] J.M. Conlon, Structural diversity and species distribution of host-defense peptides in frog skin secretions, Cell. Mol. Life Sci. 68 (2011) 2303–2315, https://doi.org/10.1007/s00018-011-0720-8.
[8] Y. Yoshimura, E. Kasuya, Odorous and non-fatal skin secretion of adult wrinkled frog (*Rana rugosa*) is effective in avoiding predation by snakes, PLoS One 8 (2013) e81280, , https://doi.org/10.1371/journal.pone.0081280.
[9] C. Jared, M.M. Antoniazzi, A.E. Jordão, J.R. Silva, H. Greven, M.T. Rodrigues, Parotoid macroglands in toad (*Rhinella jimi*): their structure and functioning in passive defence, Toxicon 54 (2009) 197–207, https://doi.org/10.1016/j.toxicon.2009.03.029.
[10] P.L. Mailho-Fontana, M.M. Antoniazzi, J.M. Sciani, D.C. Pimenta, K.C. Barbaro, C. Jared, Morphological and biochemical characterization of the cutaneous poison glands in toads (*Rhinella marina* group) from different environments, Front. Zool. 15 (2018) 46–61, https://doi.org/10.1186/s12983-018-0294-5.
[11] G. Schmeda-Hirschmann, C. Quispe, G.V. Arana, C. Theoduloz, F.A. Urra, C. Cárdenas, Antiproliferative activity and chemical composition of the venom from the Amazonian toad *Rhinella marina* (Anura: Bufonidae), Toxicon 121 (2016) 119–129, https://doi.org/10.1016/j.toxicon.2016.09.004.
[12] G. Petroselli, M. Raices, L.D. Jungblut, A.G. Pozzi, R. Erra-Balsells, MALDI-MS argininyl bufadienolide esters fingerprint from parotoid gland secretions of *Rhinella arenarum*: age, gender, and seasonal variation, J. Mass Spectrom. 53 (2018) 465–475, https://doi.org/10.1002/jms.4082.
[13] J.M. Sciani, C.B. Angeli, M.M. Antoniazzi, C. Jared, D.C. Pimenta, Differences and similarities among parotoid macrogland secretions in south American toads: a preliminary biochemical delineation, Sci. World J. 2013 (2013) 937407, https://doi.org/10.1155/2013/937407.
[14] F.A. Anjolette, F.P. Leite, K.C. Bordon, A.E.C. Azzolini, J.C. Pereira, L.S. Pereira-Crott, E.C. Arantes, Biological characterization of compounds from *Rhinella schneideri* poison that act on the complement system, J. Venom Anim. Toxins Incl. Trop. Dis. 21 (2015) 25.
[15] L.D. Rash, R.A. Morales, S. Vink, P.F. Alewood, *De novo* sequencing of peptides from the parotid secretion of the cane toad, *Bufo marinus* (*Rhinella marina*), Toxicon 57 (2011) 208–216, https://doi.org/10.1016/j.toxicon.2010.11.012.
[16] A.T. Weil, W. Davis, *Bufo alvarius*: a potent hallucinogen of animal origin, J. Ethnopharmacol. 41 (1994) 1–8.
[17] S.R. Chandramouli, K. Vasudevan, S. Harikrishnan, S.K. Dutta, S.J. Janani, R. Sharma, I. Das, R.K. Aggarwal, A new genus and species of arboreal toad with phytotelmonous larvae, from the Andaman Islands, India (Lissamphibia, Anura, Bufonidae), Zookeys 555 (2016) 57–90, https://doi.org/10.3897/zookeys.555.6522.
[18] H. Vigerelli, J.M. Sciani, C. Jared, M.M. Antoniazzi, G.M. Caporale, C. da Silva Ade, D.C. Pimenta. Bufotenine is able to block rabies virus infection in BHK-21 cells. J. Venom Anim. Toxins Incl. Trop. Dis. 20 (2014), pp. 45. doi:https://doi.org/10.1186/1678-9199-20-45. eCollection 2014.
[19] L.M. Sousa-Filho, C.D. Freitas, M.D. Lobo, A.C. Monteiro-Moreira, R.O. Silva, L.A. Santana, R.A. Ribeiro, M.H. Souza, G.P. Ferreira, A.C. Pereira, A.L. Barbosa, M.S. Lima, J.S. Oliveira, Biochemical profile, biological activities, and toxic effects of proteins in the *Rhinella schneideri* parotoid gland secretion, J. Exp. Zool. A Ecol. Genet. Physiol. 325 (2016) 511–523, https://doi.org/10.1002/jez.2035.
[20] K. Kowalski, P. Marciniak, G. Rosiński, L. Rychlik, Toxic activity and protein identification from the parotoid gland secretion of the common toad *Bufo bufo*, Comp. Biochem. Physiol. C Toxicol. Pharmacol. 205 (2018) 43–52, https://doi.org/10.1016/j.cbpc.2018.01.004.
[21] D.O.C. Mariano, M. Di Giacomo Messias, J.P. Prezotto-Neto, P.J. Spencer, D.C. Pimenta, Biochemical analyses of proteins from *Duttaphrynus melanostictus* (*Bufo melanostictus*) skin secretion: soluble protein retrieval from a viscous matrix by ion-exchange batch sample preparation, Protein J. 37 (2018) 380–389, https://doi.org/10.1007/s10930-018-9780-z.
[22] D.O.C. Mariano, M.G. Messias, P.L. Spencer, D.C. Pimenta, Duttaphrynus melanostictus parotoid macrogland secretion protein identification, J. Venom Anim.Toxins Incl. Trop. Dis. 25 (2019) 1–12 (accepted, waiting for DOI).
[23] C. Heussen, E.B. Dowdle, Electrophoretic analysis of plasminogen activators in polyacrylamide gels containing sodium dodecyl sulfate and copolymerized substrates, Anal. Biochem. 102 (1980) 196–202.
[24] M. Ashburner, C.A. Ball, J.A. Blake, D. Botstein, H. Butler, J.M. Cherry, A.P. Davis, K. Dolinski, S.S. Dwight, J.T. Eppig, M.A. Harris, D.P. Hill, L. Issel-Tarver, A. Kasarskis, S. Lewis, J.C. Matese, J.E. Richardson, M. Ringwald, G.M. Rubin, G. Sherlock, Gene ontology: tool for the unification of biology. The gene ontology consortium, Nat. Genet. 25 (2000) 25–29.
[25] S.G. Jared, C. Jared, M.I. Egami, P.L. Mailho-Fontana, M.T. Rodrigues, M.M. Antoniazzi, Functional assessment of toad parotoid macroglands: a study based on poison replacement after mechanical compression, Toxicon 87 (2014) 92–103, https://doi.org/10.1016/j.toxicon.2014.05.020.
[26] G. Delfino, D. Nosi, F. Giachi, Secretory granule-cytoplasm relationships in serous glands of anurans: ultrastructural evidence and possible functional role, Toxicon 39 (2001) 1161–1171.
[27] A. Santo, H. Zhu, Y.R. Li, Free Radicals: From Health to Disease, vol. 2, ROS, 2016, pp. 245–263 Retrieved from https://aimsci.com/ros/index.php/ros/article/view/33.
[28] M. Schieber, N.S. Chandel, ROS function in redox signaling and oxidative stress, Curr. Biol. 24 (2014) R453–R462, https://doi.org/10.1016/j.cub.2014.03.034.
[29] A.P. Schuch, V.M. Lipinski, M.B. Santos, C.P. Santos, S.S. Jardim, S.Z. Cechin, E.L. Loreto, Molecular and sensory mechanisms to mitigate sunlight-induced DNA damage in tree frog tadpoles, J. Exp. Biol. 218 (2015) 3059–3067, https://doi.org/10.1242/jeb.126672.
[30] H. Yang, X. Wang, X. Liu, J. Wu, C. Liu, W. Gong, Z. Zhao, J. Hong, D. Lin, Y. Wang, R. Lai, Antioxidant peptidomics reveals novel skin antioxidant system, Mol. Cell. Proteomics 8 (2009) 571–583, https://doi.org/10.1074/mcp.M800297-MCP200.

[31] Z. Lu, L. Zhai, H. Wang, Q. Che, D. Wang, F. Feng, Z. Zhao, H. Yu, Novel families of antimicrobial peptides with multiple functions from skin of Xizang plateau frog, *Nanorana parkeri*, Biochimie 92 (2010) 475–481, https://doi.org/10.1016/j.biochi.2010.01.025.
[32] E.A. Barbosa, A. Oliveira, A. Plácido, R. Socodato, C.C. Portugal, A.C. Mafud, A.S. Ombredane, D.C. Moreira, N. Vale, L.J. Bessa, G.A. Joanitti, C. Alves, P. Gomes, C. Delerue-Matos, Y.P. Mascarenhas, M.M. Marani, J.B. Relvas, M. Pintado, J.R.S.A. Leite, Structure and function of a novel antioxidant peptide from the skin of tropical frogs, Free Radic. Biol. Med. 115 (2018) 68–79, https://doi.org/10.1016/j.freeradbiomed.2017.11.001.
[33] I.D. Cavalcante, M.M. Antoniazzi, C. Jared, O.R. Jr Pires, J.M. Sciani, D.C. Pimenta, Venomics analyses of the skin secretion of *Dermatonotus muelleri*: preliminary proteomic and metabolomic profiling, Toxicon 130 (2017) 127–135, https://doi.org/10.1016/j.toxicon.2017.02.028.
[34] Y. Huo, R. Xv, H. Ma, J. Zhou, X. Xi, Q. Wu, J. Duan, M. Zhou, T. Chen, Identification of < 10 KD peptides in the water extraction of Venenum Bufonis from *Bufo gargarizans* using Nano LC-MS/MS and *De novo* sequencing, J. Pharm. Biomed. Anal. 157 (2018) 156–164, https://doi.org/10.1016/j.jpba.2018.05.027.
[35] M. Bloksgaard, D. Neess, N.J. Færgeman, S. Mandrup, Acyl-CoA binding protein and epidermal barrier function, Biochim. Biophys. Acta 1841 (2014) 369–376, https://doi.org/10.1016/j.bbalip.2013.09.013.
[36] D. Neess, S. Bek, H. Engelsby, S.F. Gallego, N.J. Færgeman, Long-chain acyl-CoA esters in metabolism and signaling: role of acyl-CoA binding proteins, Prog. Lipid Res. 59 (2015) 1–25, https://doi.org/10.1016/j.plipres.2015.04.001.
[37] M.M. Antoniazzi, P.R. Neves, P.L. Mailho-Fontana, M.T. Rodrigues, C. Jared, Morphology of the parotoid macroglands in *Phyllomedusa* leaf frogs, J. Zool. 291 (2013) 42–50.
[38] D. Nosi, G. Delfino, F. Quercioli, Serous cutaneous glands in anurans: fourier transform analysis of the repeating secretory granule substructure, Naturwissenschaften 100 (2013) 209–218, https://doi.org/10.1007/s00114-013-1013x.
[39] M.J. Hayes, U. Rescher, V. Gerke, S.E. Moss, Annexin-actin interactions, Traffic 5 (2004) 571–576.
[40] S.J. Popa, S.E. Stewart, K. Moreau, Unconventional secretion of annexins and galectins, Semin. Cell Dev. Biol. 83 (2018) 42–50, https://doi.org/10.1016/j.semcdb.2018.02.022.
[41] S. Schloer, D. Pajonczyk, U. Rescher, Annexins in translational research: hidden treasures to be found, Int. J. Mol. Sci. 19 (2018), https://doi.org/10.3390/ijms19061781 pii: E 1781.
[42] J. Mai, D.M. Waisman, B.F. Sloane, Cell surface complex of cathepsin B/annexin II tetramer in malignant progression, Biochim. Biophys. Acta 1477 (2000) 215–230.
[43] L.H. Farias, A.P. Rodrigues, F.T. Silveira, S.H. Seabra, R.A. DaMatta, E.M. Saraiva, E.O. Silva, Phosphatidylserine exposure and surface sugars in two *Leishmania* (Viannia) *braziliensis* strains involved in cutaneous and mucocutaneous leishmaniasis, J Infect Dis 207 (2013) 537–543, https://doi.org/10.1093/infdis/jis689.
[44] M. Yamakami, T. Yoshimori, H. Yokosawa, Tom1, a VHS domain-containing protein, interacts with tollip, ubiquitin, and clathrin, J. Biol. Chem. 278 (2003) 52865–52872.
[45] Y. Katoh, Y. Shiba, H. Mitsuhashi, Y. Yanagida, H. Takatsu, K. Nakayama, Tollip and Tom1 form a complex and recruit ubiquitin-conjugated proteins onto early endosomes, J. Biol. Chem. 279 (2004) 24435–24443.
[46] G. Ankem, S. Mitra, F. Sun, A.C. Moreno, B. Chutvirasakul, H.F. Azurmendi, L. Li, D.G. Capelluto, The C2 domain of Tollip, a toll-like receptor signalling regulator, exhibits broad preference for phosphoinositides, Biochem. J. 435 (2011) 597–608, https://doi.org/10.1042/bj20102160.
[47] D.G. Capelluto, Tollip: a multitasking protein in innate immunity and protein trafficking, Microbes Infect. 14 (2012) 140–147, https://doi.org/10.1016/j.micinf.2011.08.018.
[48] E.J.A. Kowalski, L. Li, Toll-interacting otorein in resolving and non-resolving inflammation, Front. Immunol. 8 (2017) 511, https://doi.org/10.3389/fimmu.2017.00511 (eCollection 2017).
[49] K. Prakash, D. Fournier, Evidence for the implication of the histone code in building the genome structure, Biosystems 164 (2018) 49–59, https://doi.org/10.1016/j.biosystems.2017.11.005.
[50] J.K. Seo, J. Stephenson, E.J. Noga, Multiple antibacterial histone H2B proteins are expressed in tissues of American oyster, Comp. Biochem. Physiol. B Biochem. Mol. Biol. 158 (2011) 223–229, https://doi.org/10.1016/j.cbpb.2010.11.011.
[51] J. Jodoin, M.T. Hincke, Histone H5 is a potent antimicrobial agent and a template for novel antimicrobial peptides, Sci. Rep. 8 (2018) 2411, https://doi.org/10.1038/s41598-018-20912-1.
[52] I.Y. Park, C.B. Park, M.S. Kim, S.C. Kim, Parasin I, an antimicrobial peptide derived from histone H2A in the catfish, *Parasilurus asotus*, FEBS Lett. 437 (1998) 258–262.
[53] C.B. Park, M.S. Kim, S.C. Kim, A novel antimicrobial peptide from *Bufo bufo gargarizans*, Biochem. Biophys. Res. Commun. 218 (1996) 408–413.
[54] I. Camby, M. Le Mercier, F. Lefranc, R. Kiss, Galectin-1: a small protein with major functions, Glycobiology 16 (2006) 137R–157R.
[55] M.F. Brinchmann, D.M. Patel, M.H. Iversen, The role of galectins as modulators of metabolism and inflammation, Mediators Inflamm. 2018 (2018) 9186940, https://doi.org/10.1155/2018/9186940. eCollection 2018.
[56] S.R. Stowell, C.M. Arthur, R. McBride, O. Berger, N. Razi, J. Heimburg-Molinaro, L.C. Rodrigues, J.P. Gourdine, A.J. Noll, S. von Gunten, D.F. Smith, Y.A. Knirel, J.C. Paulson, R.D. Cummings, Microbial glycan microarrays define key features of host-microbial interactions, Nat. Chem. Biol. 10 (2014) 470–476, https://doi.org/10.1038/nchembio.1525.
[57] K. Römisch, F.W. Miller, B. Dobberstein, S. High, Human autoantibodies against the 54 kDa protein of the signal recognition particle block function at multiple stages, Arthritis Res. Ther. 8 (2006) R39.
[58] R. E. Wang, Targeting heat shock proteins 70/90 and proteasome for cancer therapy, Curr. Med. Chem. 18 (2011) 4250–4264.
[59] F.U. Hartl, Molecular chaperones in cellular protein folding, Nature 38 (1996) 571–579.
[60] M.P. Mayer, B. Bukau, Hsp70 chaperones: cellular functions and molecular mechanism, Cell. Mol. Life Sci. 62 (2005) 670–684.
[61] N.P. Dantuma, C. Heinen, D. Hoogstraten, The ubiquitin receptor Rad23: at the crossroads of nucleotide excision repair and proteasomal degradation, DNA Repair 8 (2009) 449–460, https://doi.org/10.1016/j.dnarep.2009.01.005.
[62] A. Villalobo, H. Ishida, H.J. Vogel, M.W. Berchtold, Calmodulin as a protein linker and a regulator of adaptor/scaffold proteins, Biochim. Biophys. Acta 1865 (2018) 507–521, https://doi.org/10.1016/j.bbamcr.2017.12.004.
[63] S. Li, Z. Jia, X. Li, X. Geng, J. Sun, Calmodulin is a stress and immune response gene in Chinese mitten crab *Eriocheir sinensis*, Fish Shellfish Immunol. 40 (2014) 120–128, https://doi.org/10.1016/j.fsi.2014.06.027.
[64] M. da S. Libério, I.M. Bastos, O.R. Pires Júnior, W. Fontes, J.M. Santana, M.S. Castro, The crude skin secretion of the pepper frog *Leptodactylus labyrinthicus* is rich in metallo and serine peptidases, PLoS One 9 (2014) e96893, , https://doi.org/10.1371/journal.pone.0096893.
[65] B.B.P. Souza, J.L. Cardozo Fh, A.M. Murad, M.V. Prates, M.M.A. Coura, G.D. Brand, E.A. Barbosa, C.Jr. Bloch, Identification and characterization of phospholipases a (2) from the skin secretion of *Pithecopus azureus* anuran, Toxicon 167 (2019) 10–19, https://doi.org/10.1016/j.toxicon.2019.06.002.
[66] Z.C. Gu, C. Enenkel, Proteasome assembly, Cell. Mol. Life Sci. 71 (2014) 4729–4745, https://doi.org/10.1007/s00018-014-1699-8.
[67] K.B. Hendil, R. Hartmann-Petersen, Proteasomes: a complex story, Curr. Protein Pept. Sci. 5 (2004) 135–151.
[68] A.K.H. Weiss, J.R. Loeffler, K.R. Liedl, H. Gstach, P. Jansen-Dürr, The fumarylacetoacetate hydrolase (FAH) superfamily of enzymes: multifunctional enzymes from microbes to mitochondria, Biochem. Soc. Trans. 46 (2018) 295–309, https://doi.org/10.1042/BST20170518.
[69] A.M. Cuervo, Autophagy: many paths to the same end, Mol. Cell. Biochem. 263 (2004) 55–72.
[70] P. Benes, V. Vetvicka, M. Fusek, Cathepsin D - many functions of one aspartic protease, Crit. Rev. Oncol. Hematol. 68 (2008) 12–28, https://doi.org/10.1016/j.critrevonc.2008.02.008.
[71] Y. Takei, H. Higashira, T. Yamamoto, K. Hayashi, Mitogenic activity toward human breast cancer cell line MCF-7 of two bFGFs purified from sera of breast cancer patients: co-operative role of cathepsin D, Breast Cancer Res. Treat. 43 (1997) 53–63.
[72] M. Ferreras, U. Felbor, T. Lenhard, B.R. Olsen, J. Delaissé, Generation and degradation of human endostatin proteins by various proteinases, FEBS Lett. 486 (2000) 247–251.
[73] J.W. van der Stappen, A.C. Williams, R.A. Maciewicz, C. Paraskeva, Activation of cathepsin B, secreted by a colorectal cancer cell line requires low pH and is mediated by cathepsin D, Int. J. Cancer 67 (1996) 547–554.
[74] Y. Nishimura, T. Kawabata, K. Furuno, K. Kato, Evidence that aspartic proteinase is involved in the proteolytic processing event of procathepsin L in lysosomes, Arch. Biochem. Biophys. 271 (1989) 400–406.
[75] J.W. Bird, W.N. Schwartz, A.M. Spanier, Degradation of myofibrillar proteins by cathepsins B and D, Acta Biol. Med. Ger. 36 (1977) 1587–1604.
[76] J. Kos, A. Sekirnik, A. Premzl, V. Zavasnik Bergant, T. Langerholc, B. Turk, B. Werle, R. Golouh, U. Repnik, M. Jeras, V. Turk, Carboxypeptidases cathepsins X and B display distinct protein profile in human cells and tissues, Exp. Cell Res. 306 (2005) 103–113.
[77] S. Verma, R. Dixit, K.C. Pandey, Cysteine proteases: modes of activation and future prospects as pharmacological targets, Front. Pharmacol. 7 (2016) 107, https://doi.org/10.3389/fphar.2016.00107.
[78] A.I. Guce, N.E. Clark, E.N. Salgado, D.R. Ivanen, A.A. Kulminskaya, H. Brumer 3rd, S.C. Garman, Catalytic mechanism of human alpha-galactosidase, J. Biol. Chem. 285 (2010) 3625–3632, https://doi.org/10.1074/jbc.M109.060145.
[79] J.E. Gomes Júnior, D.S. Souza, R.M. Nascimento, A.L. Lima, J.A. Melo, T.L. Rocha, R.N. Miller, O.L. Franco, M.F. Grossi-de-Sa, L.R. Abreu, Purification and characterization of a liver-derived beta-N-Acetylhexosaminidase from marine mammal *Sotalia fluviatilis*, Protein J. 29 (2010) 188–194, https://doi.org/10.1007/s10930-010-9239-3.
[80] J.R. Atack, S.I. Rapoport, C.L. Varley, Characterization of inositol monophosphatase in human cerebrospinal fluid, Brain Res. 613 (1993) 305–308.
[81] P.G. Billcliff, M. Lowe, Inositol lipid phosphatases in membrane trafficking and human disease, Biochem. J. 461 (2014) 159–175, https://doi.org/10.1042/BJ20140361.
[82] R. Kelwick, L. Wagstaff, J. Decock, C. Roghi, L.S. Cooley, S.D. Robinson, H. Arnold, J. Gavrilović, D.M. Jaworski, K. Yamamoto, H. Nagase, B. Seubert, A. Krüger, D.R. Edwards, Metalloproteinase-dependent and -independent processes contribute to inhibition of breast cancer cell migration, angiogenesis and liver metastasis by a disintegrin and metalloproteinase with thrombospondin motifs-15, Int. J. Cancer 136 (2015) E14–E26, https://doi.org/10.1002/ijc.29129.
[83] R. Kelwick, I. Desanlis, G.N. Wheeler, D.R. Edwards, The ADAMTS (a Disintegrin and metalloproteinase with thrombospondin motifs) family, Genome Biol. 16 (2015) 113, https://doi.org/10.1186/s13059-015-0676-3.
[84] D. Grenier, S. Tanabe, Porphyromonas gingivalis gingipains trigger a proinflammatory response in human monocyte-derived macrophages through the p38α mitogen-activated protein kinase signal transduction pathway, Toxins 2 (2010) 341–352, https://doi.org/10.3390/toxins2030341.
[85] M.H. Bos, R.M. Camire, Procoagulant adaptation of a blood coagulation

prothrombinase-like enzyme complex in australian elapid venom, Toxins 2 (2010) 1554–1567, https://doi.org/10.3390/toxins2061554.
[86] R.L. Harrison, B.C. Bonning, Proteases as insecticidal agents, Toxins 2 (2010) 935–953, https://doi.org/10.3390/toxins2050935.
[87] D.C. Pimenta, I. Lebrun, Cryptides: buried secrets in proteins, Peptides 28 (2007) 2403–2410.
[88] K. Conceição, K. Konno, R.L. Melo, E.E. Marques, C.A. Hiruma-Lima, C. Lima, M. Richardson, D.C. Pimenta, M. Lopes-Ferreira, Orpotrin: a novel vasoconstrictor peptide from the venom of the Brazilian stingray *Potamotrygon gr. orbignyi*, Peptides 27 (2006) 3039–3046.
[89] C.A. Nicolau, P.C. Carvalho, I.L. Junqueira-de-Azevedo, A. Teixeira-Ferreira, M. Junqueira, J. Perales, A.G. Neves-Ferreira, R.H. Valente, An in-depth snake venom proteopeptidome characterization: benchmarking *Bothrops jararaca*, J. Proteomics 151 (2017) 214–231, https://doi.org/10.1016/j.jprot.2016.06.029.
[90] V. Hook, L. Funkelstein, J. Wegrzyn, S. Bark, M. Kindy, G. Hook, Cysteine cathepsins in the secretory vesicle produce active peptides: cathepsin L generates peptide neurotransmitters and cathepsin B produces beta-amyloid of Alzheimer's disease, Biochim. Biophys. Acta 1824 (2012) 89–104, https://doi.org/10.1016/j.bbapap.2011.08.015.
[91] R. Madrid, M. Pertusa, Intimacies and physiological role of the polymodal cold-sensitive ion channel TRPM8, Curr. Top. Membr. 74 (2014) 293–324, https://doi.org/10.1016/B978-0-12-800181-3.00011-7.
[92] D. Gkika, L. Lemonnier, G. Shapovalov, D. Gordienko, C. Poux, M. Bernardini, A. Bokhobza, G. Bidaux, C. Degerny, K. Verreman, B. Guarmit, M. Benahmed, Y. de Launoit, R.J. Bindels, A. Fiorio Pla, N. Prevarskaya, TRP channel-associated factors are a novel protein family that regulates TRPM8 trafficking and activity, J. Cell Biol. 208 (2015) 89–107, https://doi.org/10.1083/jcb.201402076.
[93] S. Nakjang, D.A. Ndeh, A. Wipat, D.N. Bolam, R.P. Hirt, A novel extracellular metallopeptidase domain shared by animal host-associated mutualistic and pathogenic microbes, PLoS One 7 (2012) e30287, , https://doi.org/10.1371/journal.pone.0030287.
[94] R. Tapader, D. Bose, A. Pal, YghJ, the secreted metalloprotease of pathogenic *E. coli* induces hemorrhagic fluid accumulation in mouse ileal loop, Microb. Pathog. 105 (2017) 96–99, https://doi.org/10.1016/j.micpath.2017.02.020.